

~~CONFIDENTIAL~~

Copy 6

DM 154709

NACA RM - 54K09



RESEARCH MEMORANDUM

LONG~UDINAL STABI~Y C~RACTE~TICS AT MACH NUMBERS
UP TO 0.92 OF A ~G-BODY-TAIL COMB~ATION HA~G
A ~G WITH 45° OF SWEEPBACK AND A TML
~ V~OUS VERTICAL POSITIONS

By Jack D. Stephemon, Angelo ~dettini,
ad Mph Selan

Ames Aeronautical Laboratory ~ --
Moffett Field, Calif.

CLASSIFICATION CHANGED
UNCLASSIFIED

To. _____

NACA Res also

By authority of *RU-122* Date *Nov. 8, 1957*

Am 12-19-57

CLASSIFIED DOCUMENT

This material contains information affecting the National Defense of the United States within the meaning of the espionage laws, Title 18, U.S.C., Secs. 793 and 794, the transmission or revelation of which in any manner to an unauthorized person is prohibited by law.

NATIONAL ADVISORY COMMITTEE
FOR AERONAUTICS

WASHINGTON

J=wy 28, 1955

~~CONFIDENTIAL~~



NATIONAL ADVISORY COW= FOR AERON~CS

RESEARCH MEMORANDUM

LONGITUDINAL ST~LI~ CHARAC~STICS AT MACH mERS
 ~ TO O. ~ OF A WING~BODY~TAIL COMBINATION HA~G
 A WING WITH 45° OF SWEEPBACK AND A T~L
 IN V~OUS VERTICAL POSITTONS

By Jack D. Stephenson, Angelo Bandettini,
 and Ralph Selan

SUMMARY

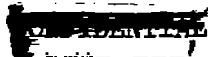
Wind-tunnel tests were conducted at Mach numbers from 0.25 to 0.92 to measure the static M@tudind stability characteristics of a semispan wing-fuselage-tail model having a w- with 45° of sweepback. The wing had an aspect ratio of 5.5 and had N~A 64A010 sections normal to the quarter-chord line. A plane, unswept, horizontal tail of aspect ratio 4 was mounted in four different vertical positions vax from 12.7-percent semispan below the wing chord plane extended to 25.5-percent semispan above the chord plane extended.

The center of pressure of the wing-fuselage combination moved forward as the wing began to stall, and a tall in the higher positions produced additional stalling moments due to high effective downwash. The bss of tail contribution due to the downwash was delayed to higher angles of attack when the tail was lowered to the wing chord plane extended.

The addition of kading-edge fences or of leading-edge chord -ens sions reduced the forward center-of-pressure movement of the wing-fusela,& combination and the losses in tail contribution that occurred when the wing stalled.

INTRomcmol!?

Existing results of aerodpic studies of w-s similar in plan form to the one employed on the model which is the subject of this report tidi- cate that the combination of plan form and section selected for this model wotid have high aerodynamic efficiency at high subsonic Mach numbers (refs. land 2). The tests reported herein were undertaken to obtati fur- ther information applicable to a complete airplane configuration suitable for superior lo~-rqe performance at high subsonic speeds. Previous tests of wings of this genera p- form indicate that at high lift coef- ficients they are subject to severe longitudinal instability as a result of an extreme forward movement of the center of pressure which results from separation of the flow at the w- tips.



~~CONFIDENTIAL~~

Tests such as those reported in references 3 and 4 of wing-body-tail combinations have shown that the contribution of the tail to the stability is of a regular nature and can generally be predicted when the wing is unstalled. However, when separation occurs on the wing, it has been observed that high downwash may occur at certain possible tail locations, causing more severe longitudinal instability than that due to the wing and fuselage. Other tail locations have been observed where the reductions in stability of the wing-fuselage combinations are partially or completely compensated for by simultaneous increases in the contribution of the tail to stability (see refs. 5 and 6).

Reference 2, which presents data from tests of a model having the wing used in the tests described in the present report and having a similar fuselage, indicates that the model was not subject to large adverse effects of compressibility on minimum drag or on maximum lift-drag ratio up to high subsonic Mach numbers. The tests reported herein were intended to ascertain to what degree the severe static longitudinal instability of the wing-fuselage combination might be avoided in the case of a model with a horizontal tail. The means of avoiding or reducing this instability included varying the vertical position of the horizontal tail and adding fences and chord extensions to the wing.

A continuing part of this program is aimed at obtaining more detailed information indicating local flow characteristics in the region of the tail of this model, which it is hoped will afford a basis for improved methods of estimating downwash behind swept wings.

NOTATION

a_t	lift-curve slope of the isolated tail
a_{wh}	lift-curve slope of the wing-fuselage combination
a_{wt}	lift-curve slope of the wing-fuse-e-tail combination
b	wing span
c	local wing chord parallel to the plane of symmetry
E	wing mean aerodynamic chord, $\frac{J b^3}{J_0}$
C_D	drag coefficient, $\frac{\text{drag}}{q_\infty}$
C_L	lift coefficient, $\frac{\text{lift}}{q_\infty}$

~~CONFIDENTIAL~~

C_m	pitching-moment coefficient about the quarter-chord point of the wing mean aerodynamic chord, $\frac{\text{pitching moment}}{\sim \%}$
i_t	incidence of the horizontal tail measured from the body center tie, deg
l	length of the body
l_t	tail length, distance from the quarter-chord point of the mean aerodynamic chord to the quarter-chord point of the horizontal-tail mean aerodynamic chord
M	free-stream Mach number
q	free-stream static pressure
q_t	effective dynamic pressure at the tail
R	Reynolds number based on wing mean aerodynamic chord
r	local radius of body
r_0	maximum radius of body
S_w	area of basic semispan wing
S_t	area of semispan tail
V_t	horizontal-tail volume, $\frac{\% Z t}{S_w \bar{c}}$
x	longitudinal distance
y	lateral distance from plane of symmetry
α	angle of attack, deg
α_t	tail angle of attack, deg
ϵ	downwash angle, deg
η	tail efficiency

MOD= AND APPARATUS

Figure 1 is a sketch of the model. The model consisted of a semispan wing, a single, a horizontal tail. The wing was constructed of solid aluminum alloy and had a 45° of sweepback at the quarter-chord line, an aspect ratio of 5.50, a taper ratio of 0.53 and was without twist. The airfoil section normal to the quarter-chord line was the NWA 64A010.

~~CONFIDENTIAL~~

The fuselage, a half-body of revolution of fineness ratio 12.5, was of cast aluminum mounted on a steel spar. The center line of the fuselage coincided with the wing-root chord line, and the quarter-chord position of the wing mean aerodynamic chord was aligned with the midpoint of the body length.

The horizontal tail surface was mounted in positions representative of possible locations of the tail on a long-range airplane. The tail volume is also believed to have been typical of such an airplane. The geometry of the tail surface was selected because its aerodynamic characteristics indicated that it would be favorable for measuring effective downwash at the tail location. A similar surface was shown in reference 7 to be free from large or erratic compressibility effects throughout the Mach number range of the model tests and to have a lift curve that was linear within a wide angle-of-attack range. The tail surface represented an all-movable stabilizer having zero sweep of the midchord line, an aspect ratio of 4.0, a taper ratio of 0.5, and NACA 63A00b sections. The tail area was 24.8 percent of the wing area and the quarter-chord point of the tail mean aerodynamic chord was 2.06 behind the quarter-chord point of the wing mean aerodynamic chord. Provision was made to mount the horizontal tail at four vertical positions, as follows: (a) a low position 17.7 percent of the wing semispan below the wing chord plane extended; (b) center position in the wing chord plane extended; (c) a medium high position 12.7-percent semispan above the wing chord plane extended; and (d) a high position 25.5-percent semispan above the wing chord plane extended. The tail surface was supported in the three positions away from the fuselage center line by means of steel pylons. The junctures between the stabilizer and pylon were covered with a wood fairing as shown in figure 2(a). When the tail was mounted below the fuselage, an additional fairing was installed over the pylon surface between the juncture fairing and the fuselage (fig. 2(b)) in an effort to reduce interference at high angles of attack.

The fences shown in figure 1(b) were mounted on the wing during portions of the test at one or more of the following spanwise stations: $0.44b/2$, $0.57b/2$, $0.69b/2$, and $0.82b/2$. Figure 2(c) is a photograph of one combination of the fences. Provision was made for testing the fences with the rearward 70 percent or 80 percent removed. Leading-edge chord extensions were also installed on the outer portion of the wing during part of the test. These extensions (shown in figs. 1(b) and 2(d)) increased the local chord normal to the quarter-chord line by 15 percent and increased the streamwise chord by 17 percent. The inner ends of the chord extensions, which were located as indicated in figure 1(b), were plane surfaces parallel to the model plane of symmetry. The chord-extension section was similar to the forward part of the original section, except for a reduced thickness ratio and nose radius, and was faired into the basic wing section at its maximum thickness. Coordinates of the chord extensions in sections normal to the quarter-chord line of the original wing are given in table I. The wing area of the model was increased by 8 percent when the largest chord extension was installed.

~~CONFIDENTIAL~~

~~CONFIDENTIAL~~

Additional "geometric data are listed in table ~ for the various model components.

a m

~erimental studies were conducted to determine the static tingi-
tudinal stability characteristics of the model without the tail and with
the tail mounted at each of the four positions indicated in figure 1.
With the tail at the fuselage center line and 12.7-percent semispan above
the center ~, its incidence was varied from 0° to -5°.

Effects of various fence installations upon the characteristics of
the wing-fusekge combination were measured in a limited series of tests
and one fence configuration was s~ected for more detaibd stability
studies. The effects of kading-edge chord tiensions upon the longitu-
dinal stability of the model were -so investigated.

Measurements were made of I-ift, drag, md pitc~ moments at Mach
numbers from 0.5 to 0.92 at a Reynolds number of 2,000,000. At a Mach
number of 0.25, data were also obtained at a Reynolds number of 10,000,~0.

CO=TIONS TO DATA

The data have been correctid for constriction effects due to the
presence af the tunnel walls, for tunnel-w~ interfe=nce effects origi-
nating from lift ~n the model, and for the drag tares caused by aerodw=ic
forces on the exposed portion of the turntable on which the model was
mounted.

The dynamic pressure and the Mach number were co-netted for constrict-
tion effects due to the presence of the tunnel walls by the methods of
reference 8. The corrected and uncorrected Mach numbers =d the ratio of
corrected to uncorrected dynamic pressure are presented in table III(a).
The correction to the drag coefficient for the effect of the pressure
gradient due to the wake was esttiated and found to be negligible.

Corrections for the effects of tunnel-wall interference due to mode 1
lift were calculated by the method of reference 9. The corrections (which
were added t~ the data) were as fo~ws:

$$\begin{array}{lll} A_m = K_1 C_L & A_{C_m} = K_2 C_L & \text{Model without tail} \\ A_{CD} = 0.0053 C_L^2 & A_{C_m} = \& C_L & \text{Model with tail} \end{array}$$

The values of K_1 , K_2 , and K_3 are shown h table III(b) as functions of
Mach number.

~~CONFIDENTIAL~~

Since the turntable upon which the model was mounted was directly connected to the balance system, a tare correction to the drag was necessary. The magnitude of this correction was calculated by multiplying the forces on the turntable with the model removed the drag of the area of the turntable exposed to the air stream after installation of the model. The tare corrections, converted to tare drag coefficients based on wing area, were subtracted from the measured drag coefficients and are presented in table 1(c). No attempt has been made to evaluate tares due to interference between the model and the turntable or to compensate for the tunnel-floor boundary layer, which at the turntable had a displacement thickness of one-half inch.

RESULTS ~ DISCUSSION

Basic Model

The lift, drag, and moment characteristics of the wing-fuselage combination are presented in figures 3 and 4. The data are practically identical to those measured on a similar wing-body combination and reported in reference 2. Throughout the test range of Reynolds numbers and Mach numbers and at lift coefficients greater than about 0.6, the center of pressure of the wing-body combination moved forward rapidly with increasing angle of attack. As is well known, this behavior is a result of flow separation beginning at the wingtip and progressing inward with increasing angle of attack and is characteristic of wings of this general plan form. In addition to the data for the wing-fuselage combination, data are presented for the model with the three tail-mounting pylons and fairings, which, except for increasing slightly the level of the drag data, had only minor effects. Small differences in pitching moments for various tail-mounting pylons can be attributed to the fact that the characteristics at the stall were somewhat erratic and not repeatable.

Figures 5 and 6 show the effects of adding the horizontal-tail surface in various vertical positions. The pitching-moment data referred to the wing quarter-chord point indicate a considerable static margin for the angle-of-attack range where the lift curve remained linear. At the higher angles of attack, large and abrupt movements of the center of pressure occurred. These movements were greatest when the tail was in the highest position and decreased progressively as the tail was lowered. A detailed comparison of the pitching moments of the model with and without the tail (figs. 3 through 6) indicates that when the tail was 12.7-percent semispan below the fuselage, it contributed to the stability throughout the angle-of-attack range, whereas for higher tail locations, when stalling occurred, the tail contributed a powerful positive pitching moment.

me decreased static longitudinal stability near zero lift for the model with the tail at the fuselage center line is an indication of the effect of the wing area. The data show that the pitching moment at zero lift varied with tail height, indicating a local flow at the tail directed inward toward the fuselage.

Effect of Fences

The effect of the location of half-chord fences was investigated at two Mach numbers by installing the fences in several combinations at one or more of the following stations: $0.44b/2$, $0.57b/2$, $0.69b/2$, and $0.82b/2$. The lift and moment characteristics of the model without the tail (fig. 7(a)) indicate that at a Mach number of 0.9 a single fence at 44-percent semispan increased the lift coefficients at which large forward center-of-pressure movements occurred and reduced the magnitude of these movements prior to the attainment of maximum lift. The least variation of center of pressure with lift coefficient resulted when two fences were used, one at 44-percent and one at 69-percent semispan. None of the fence combinations provided any substantial improvements at a Mach number of 0.9. It was noted that some insight into the origin of the improved stability due to the fences might be afforded if the chordwise extent of the fences were varied. Results of tests with two fences (at 44-percent and 69-percent semispan) having the after fence at 50 percent and the after 50 percent of the fences removed are presented in figure 7(b). The data show that fences extending over only the forward 50 percent of the chord were almost as effective as any of the longer chord fences, indicating that the effects of separation on this wing were most strongly influenced by the flow near the leading edge. The full-chord fences resulted in slightly higher values for the lift coefficient at which the center of pressure moved forward. On the basis of these limited tests of the model without the tail, the full-chord fences at 0.44 and 0.69 semispan were selected to be tested in more detail.

The lift, drag, and moment characteristics of the model without the tail and with full-chord fences at 0.44 and 0.69 semispan are shown in figure 8 at Mach numbers from 0.25 to 0.92 and a Reynolds number of 2,000,000. At all these Mach numbers the fences reduced the forward center-of-pressure movement accompanying stalling of the wing (prior to maximum lift) and at Mach numbers up to 0.92 substantially increased the lift coefficient at which instability occurred. The addition of the fences had very slight effect on the minimum drag and reduced the drag at moderate and high lift coefficients. At a Mach number of 0.92 there was some drag penalty due to the addition of fences.

Figure 9 shows the longitudinal characteristics of the model with fences and the various tail pylons at a Reynolds number of 10,000,000 and a Mach number of 0.9. Similar data for the Mach number range 0.25 to 0.92

~~CONFIDENTIAL~~

~~CONFIDENTIAL~~

at a Reynolds number of 2,000,000 are pre-specified in Figure 20. Comparison with the same type of data for the model without fences (figs. 3 and 4) indicates that the incursions in the pitching-moment characteristics at the stall were somewhat reduced by the addition of fences.

Data for the model with fences and with the tail in various vertical positions are presented in figures 11 and 12 for Reynolds numbers of 10,000,000 and 2,000,000, respectively. With the tail in the high position, longitudinal instability occurred at angles of attack where the wing was partially stalled (as indicated by decreased lift-coefficient slopes). Raising the tail decreased the magnitude of the instability and increased the angle of attack where it first occurred. With the tail in the chord plane extended, there were relatively small variations with lift coefficient of the center-of-pressure location, and the pitching-moment curves were considerably more linear than those for the model without fences. The improved stability for the higher tail positions was partly due to the effect mentioned previously of the fences on the stability of the wing-body combination. A detailed examination of the pitching moments of the model with fences both with and without the tail (figs. 9 through 12) has indicated that the tail did not contribute the large positive pitching moments which were observed for the model without fences, when the wing was partially stalled. Although the model was generally stable at maximum lift (in those cases when it was stalled), with the tail in the two lower positions there was an abrupt change in pitching moment at high angles of attack prior to maximum lift. This is believed to have been due to stalling of the tail. Such stalling probably does not represent a flight problem for an airplane with a center-of-gravity location that would normally be employed because of the decrease in tail incidence that "would be necessary for longitudinal balance in flight at these lift coefficients."

Effects of Chord Extensions

The lift and moment data measured at a Mach number of 0.8 and a Reynolds number of 2,000,000 are presented in figure 13 for the wing-fuselage model with chord extensions of various spans. The greatest improvement in linearity of the pitching-moment data resulted when the leading-edge discontinuity was at the innermost location. The addition of a fence at this discontinuity produced no improvement. The effects of increased Mach number on the characteristics of the wing-fuselage combination with the two longest span chord extensions are shown in figure 14. The pitching-moment characteristics of the wing-fuselage model with chord extensions were similar to the characteristics of the model with fences. At Mach numbers up to 0.85, there were substantial increases in the lift coefficients where large center-of-pressure moments occurred, but at Mach numbers of 0.90 and 0.92, only slight increases in the lift coefficients are evident. Although the increased wing area due to adding the chord extensions increased the lift proportionately, this effect

~~CONFIDENTIAL~~

~~CONFIDENTIAL~~

accounts for less than a sixth of the measured increase in the lift coefficient at which longitudinal instability occurred at the lower speeds.

In order to determine whether the downwash at the tail would be significantly influenced by the span of the chord extension, tests were conducted with two of the more promising chord extensions, one extending from 44-percent semispan to the wing tip and the other from 57-percent semispan to the tip. As shown in figures 15 and 16, with the tail in the wing chord position, large forward movements of the center of pressure were avoided almost up to the wing maximum lift when either of these chord extensions was employed. Raising the tail to the medium position (0.127b/2) had adverse effects upon the stability, particularly with the shorter span chord extension. The addition of the longer span chord extension resulted in stability characteristics of the complete model quite similar to those of the model with fences. Because there was no clear superiority in the characteristics of the model with chord extensions over those of the model with fences, this modification was not studied in more detail. The possibility exists that one wing leading-edge modification may have some advantage in drag over the other modifications, but it is believed that the tests reported herein are inconclusive in this respect because the method of attaching the fences (fig. 2(c)) is certainly not optimum from the drag standpoint and because the basic-wing drag may have varied when the surface conditions were not sufficiently well duplicated each time the chord extensions were installed or removed.

Effectiveness of the Tail as an U-Movable Control

Figures 17 and 18 present data showing the effects of varying the tail incidence on the model without fences or chord extensions. At a Reynolds number of 10,000,000 (and Mach number of 0.5) figure 17 shows that varying the tail incidence from 0° to -5° was effective in varying the pitching moment at all angles of attack below maximum lift. Throughout the Mach number range at a Reynolds number of 25,000,000 (fig. 18) the stabilizer provided effective control until the effects of wing stalling upon the stability became large.

With two full-chord fences on the model, the data presented in figures 19 and 20 indicate that the stabilizer was effective until the wing stalled, but the effectiveness at the stall was erratic in some instances. Abrupt forward movements of the center of pressure occurred near maximum lift at some Mach numbers, but the study of such movements was small when the tail incidence was -5° .

~~CONFIDENTIAL~~

Characteristics at k Lift Coefficients

The slope of the H_t and pitching-moment curves and the variation of pitching-moment coefficient with stabilizer angle derived from data in the preceding figures are shown in figure 21. This figure shows m/\bar{L} of the model without the tail at a lift coefficient of 0.1. This lift coefficient was selected to indicate the slope of the moment curve at low angles of attack and still avoid a discontinuity in the slope that characterized the data near zero lift at the higher Mach numbers with the tail off. Adding the fences caused the rearward movement of the aerodynamic center of the wing-fuselage combination at low angles of attack to occur at a lower Mach number. Data showing dC_m/dC_L of the complete model indicate that raising the tail from the fuselage center line to the medium (0.127b/2) position increased the static stability at zero lift. Adding fences produced no consistent effect on the stability of the complete model at zero lift. The stabilizer effectiveness U_{dit} at zero angle of attack shown in figure 21 as a function of Mach number indicates that increasing Mach number produced generally higher effectiveness, particularly when the tail was in the medium high location.

Tail Contribution to Stability

The force and pitching-moment data for the model with the medium and center-line tail locations (figs. 17 through 20) have been used to estimate the effective downwash angles shown in figures 21 and 23 as functions of angle of attack. (In order to estimate the downwash at high angles of attack, it was necessary to assume that the stabilizer effectiveness data could be extrapolated to include negative angles of incidence of the tail that were beyond the range of the experimental data.)

In figure 22 and at the top of figure 23 the effective downwash data at a Mach number of 0.25 are shown at two Reynolds numbers, 10,000 and 2,000,000, respectively. At both Reynolds numbers, the slopes of the downwash curves for the model without fences increased sharply at angles of attack slightly exceeding those where wing-body instability occurred. At all of the Mach numbers of the test (at a Reynolds number of 2,000,000) the slope of the downwash curves increased with angle of attack, but, when the tail was lowered to the center line, this increase was delayed to higher angles of attack (see fig. 23). The effects of adding fences are also shown in figures 22 and 23: the most significant effect was to decrease the downwash at the higher angles of attack, particularly in the region of the medium tail.

Force and pitching-moment data for the model with and without the tail, and force data for the isolated tail have been used to calculate the contribution of the horizontal tail to the longitudinal stability, as expressed in the following formula.

$$\left(\frac{dC_m}{dC_L}\right)_t = -V_t \frac{a_t}{a_{w+b}} \left[\eta \frac{q_t}{q} \left(1 - \frac{d\epsilon}{d\alpha}\right) + \alpha_t \frac{\partial \left(\eta \frac{q_t}{q}\right)}{\partial \alpha} \right]$$

This expression for the tail stability parameter $(dC_m/dC_L)_t$, where ϵ is the variation of pitching-moment coefficient due to the tail with lift coefficient of the wing-fuselage combination, affords a useful indication of the way the separate factors affect the tail contribution to the pitching moment of the model. This parameter is related to the increment due to the tail in the stability of the complete model by the expression

$$\left(\frac{dC_{m_t}}{dC_L}\right)_{w+b+t} = \frac{a_{w+b}}{a_{w+b+t}} \left(\frac{dC_m}{dC_L}\right)_t$$

The terms in the expression for the tail stability parameter were evaluated as follows: the lift-curve slope of the isolated tail a_t was obtained from references 7 and 10 was measured at the average effective tail angle of attack as indicated by the effective downwash data. It was assumed that the Mach number at the tail was the same as the free-stream Mach number. The lift-curve slope of the wing-fuselage combination a_{w+b} was measured from data presented in figures 3, 4, 9, and 10. The product of the tail efficiency and the dynamic pressure at the tail $\eta(q_t/q)$ was computed from the relation $\eta(q_t/q) = \frac{dC_{dit}}{V_t a_t}$ where dC_{dit} is the stabilizer effectiveness measured at constant model angle of attack. In

calculating the tail contribution, the term $\frac{\partial \left(\eta \frac{q_t}{q}\right)}{\partial \alpha}$ was neglected.

The variations of the tail contribution to the stability and the factors making up this contribution are shown in figure 24 for a Reynolds number of 10,000,000 and a Mach number of 0.5, and in figure 25 for a Reynolds number of 2,000,000 and Mach numbers of 0.6, 0.8, and 0.9. Although the factor a_{w+b} and the tail efficiency and dynamic pressure factors indicated sizable variations with angle of attack for all the conditions shown, they did not appear to be of major importance in determining the effect of the vertical location of the tail. A comparison of the variations with angle of attack of the downwash factor $(1 - d\epsilon/d\alpha)$

and the tail stability parameter ($dC_{L}/d\alpha$) indicates that practically all of the significant characteristics of the latter can be traced to variations in downwash. At W_{ch} numbers at least up to 0.9, rapid increase of effective downwash at the tail with increasing angle of attack resulted in decreased contribution of the tail to stability. When the tail was lowered from the medium to the center position, this decrease was delayed to higher angles.

The effects of adding fences to the model were to reduce or eliminate large erratic variations of ($dC_{L}/d\alpha$) at high angles of attack and under some of the test conditions to eliminate a loss of tail contribution that occurred as the wing first began to stall. This loss in tail contribution for the model without fences is the most noticeable in the data for the medium tail height and was still present to a lesser degree when fences were installed. At each of the test conditions shown, when such a loss occurred, it was diminished or avoided by lowering the tail to the model center line.

The large variations that are apparent in the factor $(1 - dC_{L}/d\alpha)$ may give rise to speculation as to the accuracy of such data, in view of the difficulty in calculating effective downwash from data in which the pitching moments are erratic. Although large and abrupt changes in the pitching-moment coefficient were measured when stalling of the wing occurred, it is believed that by careful examination of the moment data it has been possible to determine effective downwash angles that are at least qualitatively reliable and do not include important effects of dispersion or other inaccuracies.

Figure 25 includes some values of $q(qt/q)$ which appear to be too high, exceeding unity at Mach numbers of 0.6 and 0.8 at high angles of attack. These values were calculated at conditions where the tail was at high angles of attack and may be in error as a result of factors that could not be properly accounted for in the method of calculation used. The pitching-moment data indicate that the tail was more effective at high angles of attack than would be predicted from estimates based on the lift curve of the isolated tail. The differences appear to result from differences in the shape of the Wt curves of the tail when it was on the model as compared to the isolated tail, and are probably associated with local characteristics of the flow in the vicinity of the tail, such as the spanwise distribution of the downwash and the turbulence level of the flow near the tail. It is believed that the data presented for these angles of attack still provide a valid indication, at least qualitatively, of variations in tail contribution to pitching moment and the factors that most affect it.

Tail Incidence for Balance

Figure 26 shows the tail incidence required for longitudinal balance as a function of lift coefficient for the model with the tail in the chord plane extended (center position) and in the medium position. The center of gravity was in all cases assumed to be at 44 percent of the mean aerodynamic chord. This location was selected as the most rearward point at which a static margin of 5-percent mean aerodynamic chord could be maintained throughout the range of Mach numbers at low to moderate angles of attack and was governed by the stability characteristics of the model with the tail at the center location.

The severe instability of the model without fences and with the tail 0.075 above the \sim chord plane is evidenced by the large positive incidence angles required for balance at lift coefficients near 0.9. These positive angles of incidence were estimated by extrapolating the data, since the tests included only negative and neutral settings of the tail. The data show that adding the fences had considerable effect in decreasing the magnitude of the instability and in reducing the range of CL for which the instability occurred. When the tail was in the center position and with the center of gravity at 0.44, the model with fences was stable at \sim the Mach numbers of the tests and at all lift coefficients, except just prior to the attainment of maximum lift. It would be expected that other tail locations above the center but lower than the medium tail would also result in longitudinal stability under all these conditions.

In selecting the vertical location of the horizontal-tail surface on an airplane, considerations of ground clearance in the landing attitude, distance from the jet exhaust, and the vertical location and incidence of the wing relative to the fuselage often require that the tail be above the wing chord plane. Further tests would be desirable to determine the highest position where a tail might be mounted behind a wing similar to the one that is the subject of this report, so as to provide adequate stability throughout the range of speeds and altitudes that would be encountered in flight.

CONCLUSIONS

Wind-tunnel tests of a wing-fuselage-tail combination having a tail swept back 45° and an aspect ratio of 5.5 indicated the following conclusions.

1. A large and abrupt forward movement of the center of pressure of the wing-fuselage combination at high angles of attack was a source of static longitudinal instability of the complete model. When a tail was

~~CONFIDENTIAL~~

added to the model in a position below the wing chord plane, the significant variations in stability at high angles of attack were still attributable to the wing-fuselage characteristics, but as the tail height was progressively increased to 0.255 semispan above the wing chord plane, the tail produced increasingly powerful positive pitching moments.

2. For the model both with and without the tail, leading-edge fences at 4-percent and 69-percent semispan reduced the forward movement accompanying stall of the wing (prior to maximum lift) and, at Mach numbers up to 0.85, substantially increased the lift coefficient at which instability occurred.

3. A leading-edge chord extension between the wing tip and the 44-percent semispan station resulted in an improvement in stability that was similar to that provided by the leading-edge fence.

4. At Mach numbers up to 0.9, rapid increase of effective downwash at the tail with increasing angle of attack resulted in decreased contribution of the tail to stability, but when the tail was moved to the wing chord plane this decrease was delayed to higher angles of attack.

5. The effects of adding fences were to reduce or eliminate the decrease in the contribution of the tail to stability.

6. Significant variations of static longitudinal stability with lift coefficient are indicated in data for the model configurations investigated, but the model with fences and with the tail near the wing chord plane would be stable at all of the Mach numbers of the test and at all lift coefficients (except those at or just prior to maximum lift) if the center of gravity were located so as to provide a minimum static margin at low angles of attack of 5 percent of the aerodynamic chord.

Ames Aeronautical Laboratory
National Advisory Committee for Aeronautics
Moffett Field, Calif., Nov. 9, 1954

REFERENCES

1. Johnson, Ben H., Jr., and Shibata, Harry H.: Characteristics Throughout the Subsonic Speed Range of a Plane Wing and of a Cambered and Twisted Wing, Both Having 45° of Sweepback. NACARM A5-27, 1951.
2. Shibata, Harry H., Bandettini, Angelo, and Cleary, Joseph: An Investigation Throughout the Subsonic Speed Range of a Half-Span and a Semispan Model of a Plane Wing and a Cambered and Twisted Wing, all Having 45° of Sweepback. NACA A52-152, 1952.

~~CONFIDENTIAL~~

3. Bandettini, Angelo, and Seb, Ralph: The Effects of Horizontal-Tail Height and a Parti--Span ~ading-Edge Wension on the Static kngitudi~ Stability of a Wing-Fuselage-Tail Combination Having a Sweptback Wing. NACA RM A5~07, 1%4.
4. Tifiing, Bruce E.: The bngitudinal Characteristics at Mach Numbers up to 0.9 of a Wing-Fuselage-Tail Combination Having a Wing With 40° of Sweepback and an Apect Ratio of 10. NACA RM A5=19, 1952.
- 5- Foster, GeraU V., and Griner, Roland F. : hw-Speed kngitudinal and Wake Air-Fh Characteristics at a ReynoHe Ntier of 5.~x10⁸ of a Circular-Arc 52° Sweptback Wing With a Fuselage ada Horizontal Tail at Various Vertical Positions. NACA RM L51C30, 1%1.
6. Salmi, Reino J., and Jacques, Willi- A.: Effect of Vertical kcation of a Horizontal Tail on the Static tingitudinal Stability Charac-teristics of a 45° Sweptback Wing Fuselage Combination of Aspect Ratio 8 at a Re~olds Nmber of 4.0xl&. NACARM L~1J@, 1952.
7. Nelson, Warren H., ~len, Edwin C., and ~, Walter J.: The Tran-sonic Characteristics of 36 S~etricd Wings of Varying Taper, Aspect Ratio, and Thickness as Determinedly the Transonic-BumQ Technique. NACARMA53129, 1953.
8. Herriot, Jok G.: Blockage Corrections for Three-Dimensional-Flow Closed-Throat Wind Tunnels With Consideration of the Effect of Compressibility. NACA Rep. ~, 1~0. (Former~NACA~ A7B28).
9. Sive~s, James C., and Salmi, Rachel M.: Jet-Boun@ Corrections for Complete and Semisp= Swept Wings in Closed Circular Wind Tunnels. NACATN 24Y4, 1%1.
10. Cahill, Jones F., and GottUeb, Stdey M.: --Speed Aerodynamic Characteristics of a Series of Swept Wings Having NACA65A006 ~r-foil Sections. NACARM L9J20, 1~0.

~~CONFIDENTIAL~~

TAB~ I.- COORDINA~ OF CEORD--ION SECTION NO- TO
 QUARTER-CHORD L~
 [All dtiensions in percent of chord of original section]

Station	Otiinate
-15.0	o
-14.3	.80
-13.9	1.00
-13.0	1.30
-11.9	1.60
-10.0	2.00
-7.0	2.50
-3.0	3.00
	::;
17.0	4:50
'25.3	4.80
35.1	4.97
40.0	5.00


 NACA
~~CONFIDENTIAL~~

TABLE II. - G~ OF ~ MODEL

Wing (without kading-edge e-nsion)	
Aspect ratio	5.50
Taper ratio	0.532
Sweep of quarter-chord line, deg	45
Section normal to quarter-chord line	NACA 64A010
Area (semispan), sqft	3.812
Meanaerodyn=ic chord, ft	1.215
Dihedral	0
hcidence	0
Positiononbody	on =is
Wing leading-edge chord extension	
Streamwise distance to extended leading edge	0.17c
hcations of inboard ends of extensions	0.44b/2, 0.57b/2, o.6gb/2, o.82b/2
Wing fences	
Distance aheadofwingkading edge	0.*C
Spanwiselocations	0.4hb/2, 0.57b/2, o.69b/2, o.82b/2
Chordwise extent (from leading edge)	0.25c, 0.50c, 1.00c
Fuselage	
Fineness ratio	12.5
kn@h,ft	7.292
Frontdarea/tingarea	0.035
Horizontal tail	
Aspect ratio	4.0
Taper ratio	0.5
Sweep, deg (50.p~rcent chord)	
Section	N~A 63A00!
Area (setispansqft)	0.945
Tail length(Zt)	= 2.0E
Vertical distance above wing chord ptie extended	
kwtail	- - - -0. E7b/2
Center tail	
Medium tail	0. =7b/:
Hightail	0. 255b/2

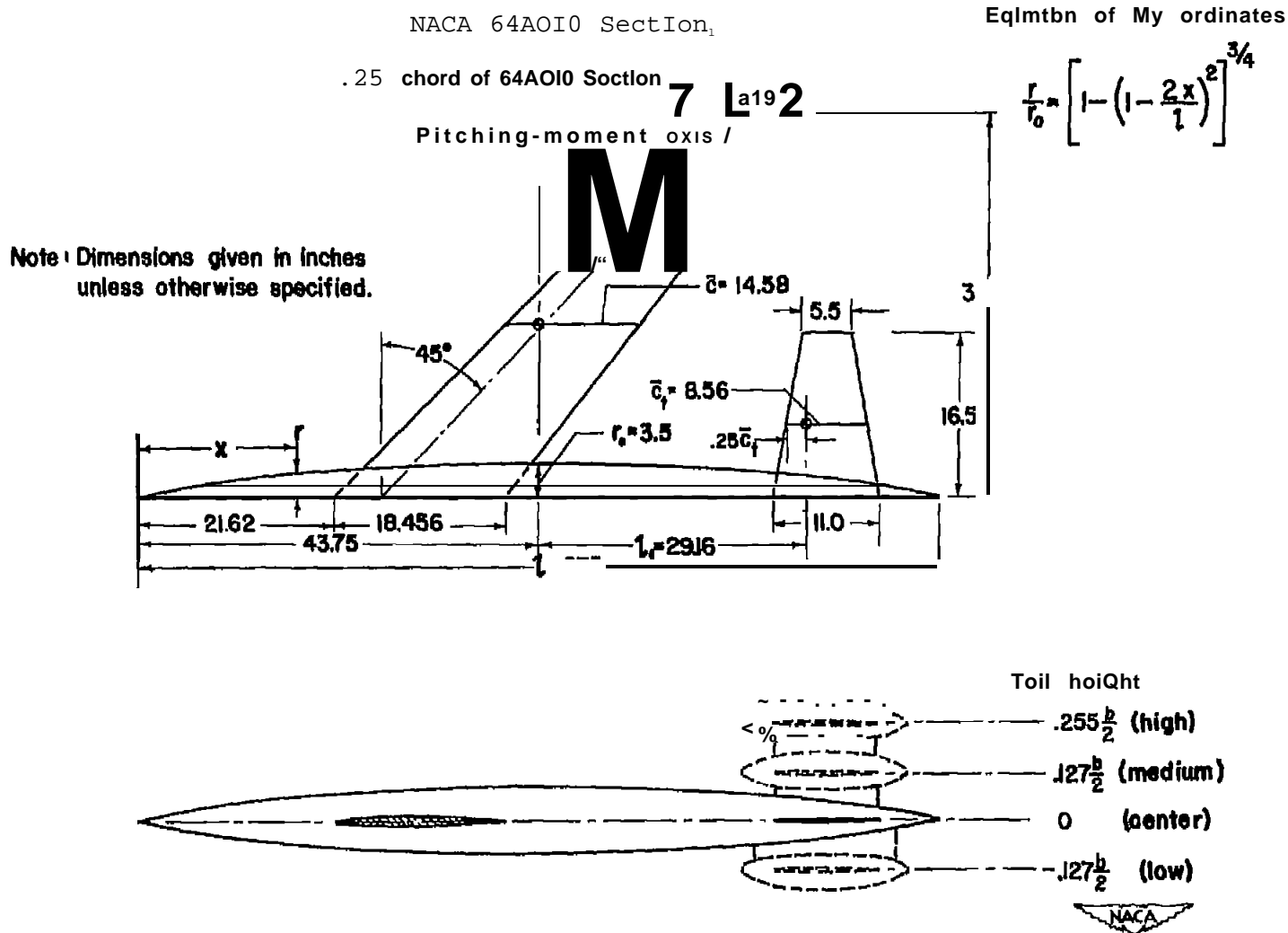
~~CONFIDENTIAL~~

Tm ~ ~ . - CORRECTIONS TO DATA

(a) Constriction due to tunnel walls		
Corrected Mach number	Uncorrected Mach number	qcorrected
		quncorrected
0.25	0.250	1.001
~:	.399	1.002
	* 797	1.004
: ?	.846	1.00m
	.893	1.008
.92	.911	1.010
(b) Jet-bound- effects		
~	$K = \frac{Aa}{CL}$ (wing body)	$\& = \frac{A}{q} +$ (wing body tail)
0:5	0.349	0.0038
	.349	.0052
	.349	.0080
::5	.349	.00~
	; :::	.0114
"::2	.0001	.0123
(c) Tare corrections		
Repolda number	Mach nutnber	c=tare
10,000,000	0. -	0.0049
2,000,000	.25	.00@o
2,000,000	.60	. C)ql
2,m,ooo	.80	.0057
2,000,000	.85	. OMO
2,000,000	.90	.0064
2,000,000	.92	.0067

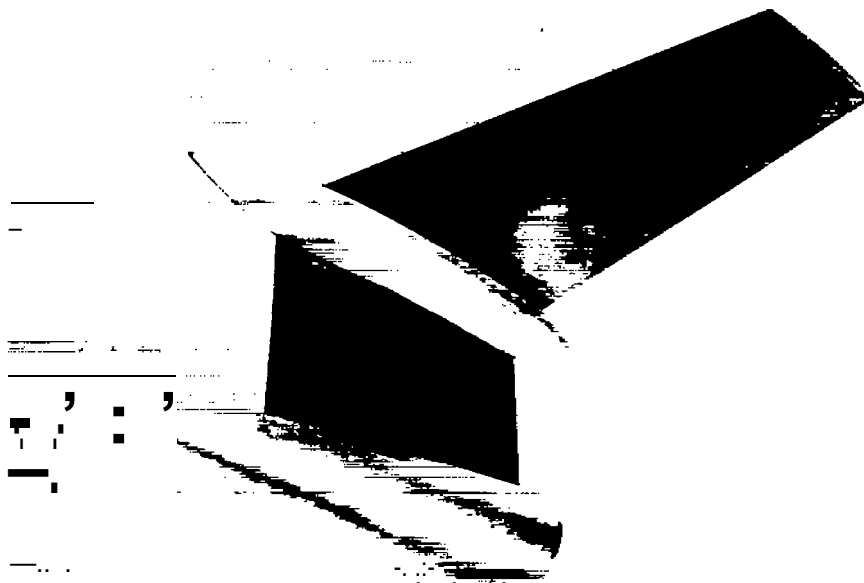
~

~~CONFIDENTIAL~~



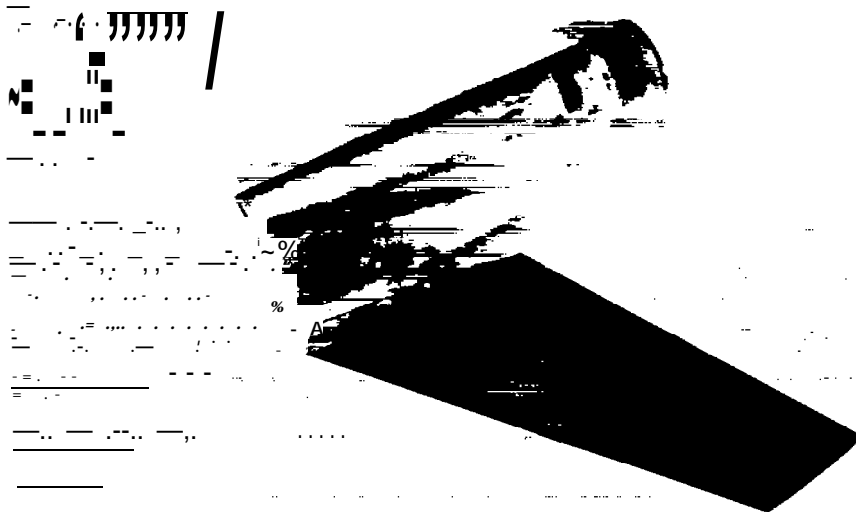
(a) Complete model and W1 helix.

Figure 1,- Draw of the model.



A-19237.1

(a) High tail position.



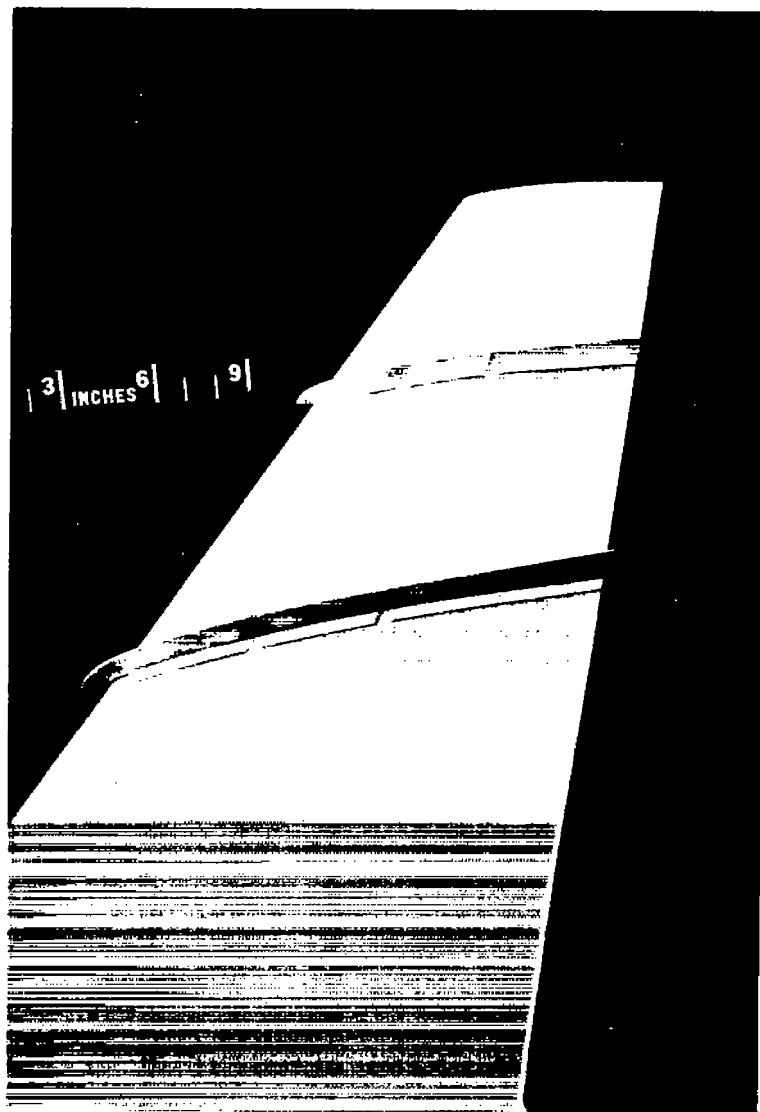
A-19238.1

(b) Low tail position.

Figure 2.- Photographs of the model.

~~CONFIDENTIAL~~

-----NACA RM A54K09



A-1q1'82

(c) Full-chord fences at $0.5b/2$ and $0.6gb/2$.

Figure 2.- Continued.

~~CONFIDENTIAL~~

CONFIDENTIAL

A-18987

(d) Model with a leading-edge chord definition between $0.44b/2$ and the tip.

Figure 2.- CONC~d~.

CONFIDENTIAL

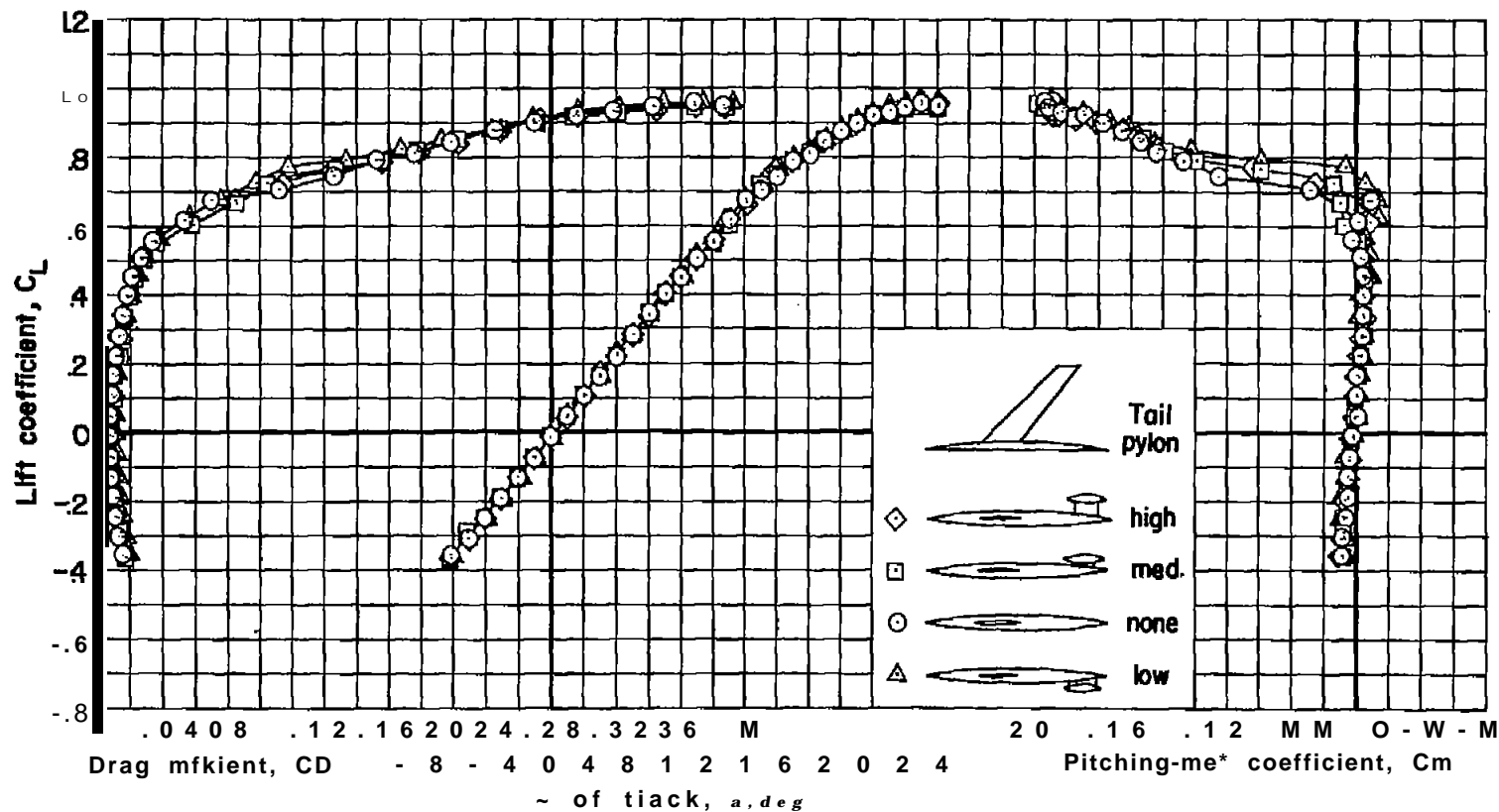


Figure 3.- aerodynamic characteristics of the model with the tail off and with various tail Bupoti pylons at a Reynolds number of 10, 000; $M = 0.2$.

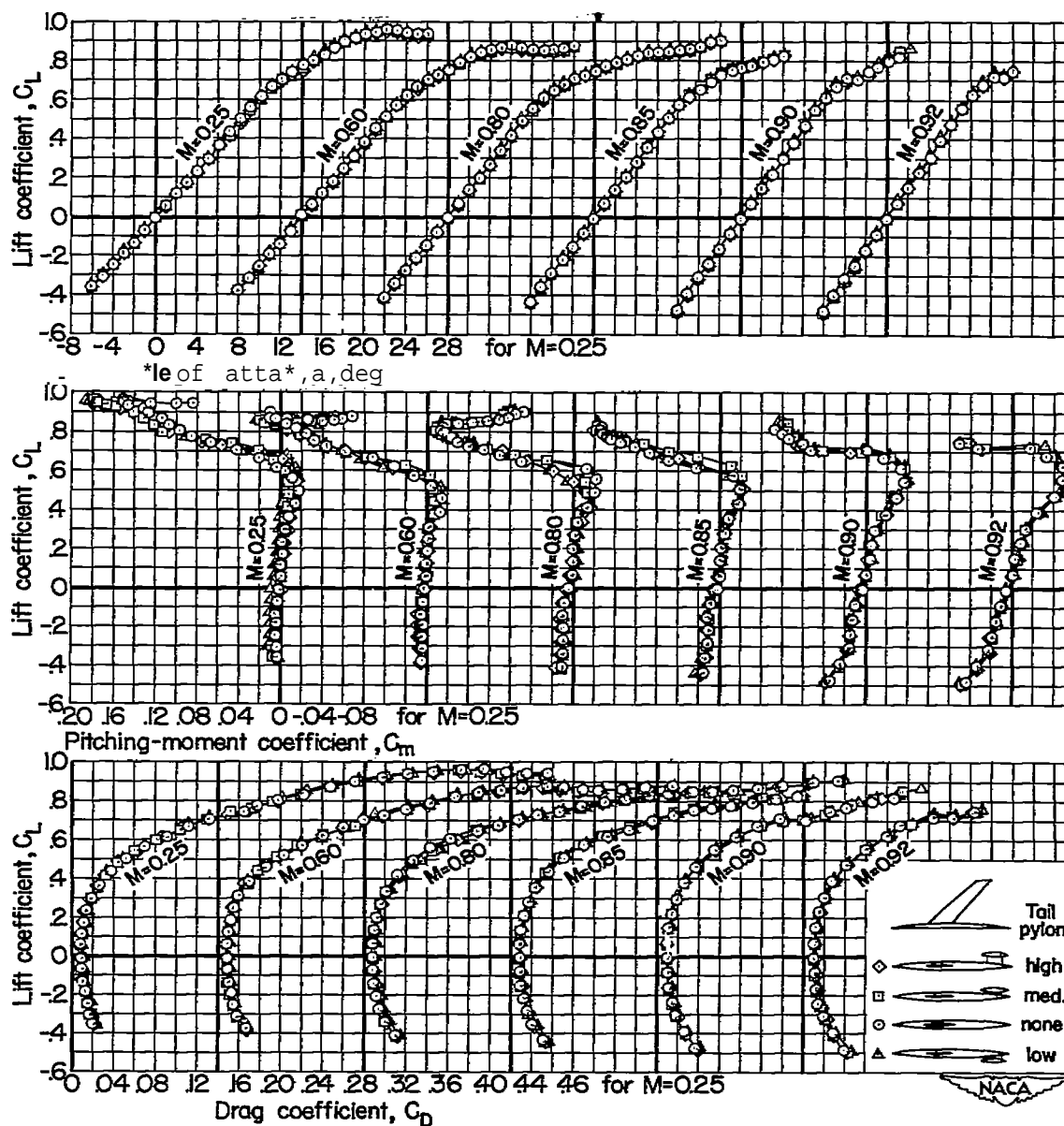


Figure 4.- aerodynamic characteristics of the model with the tail off
 @ with various tail support pylons at several Mach numbers;
 $R = 2,000,000$.

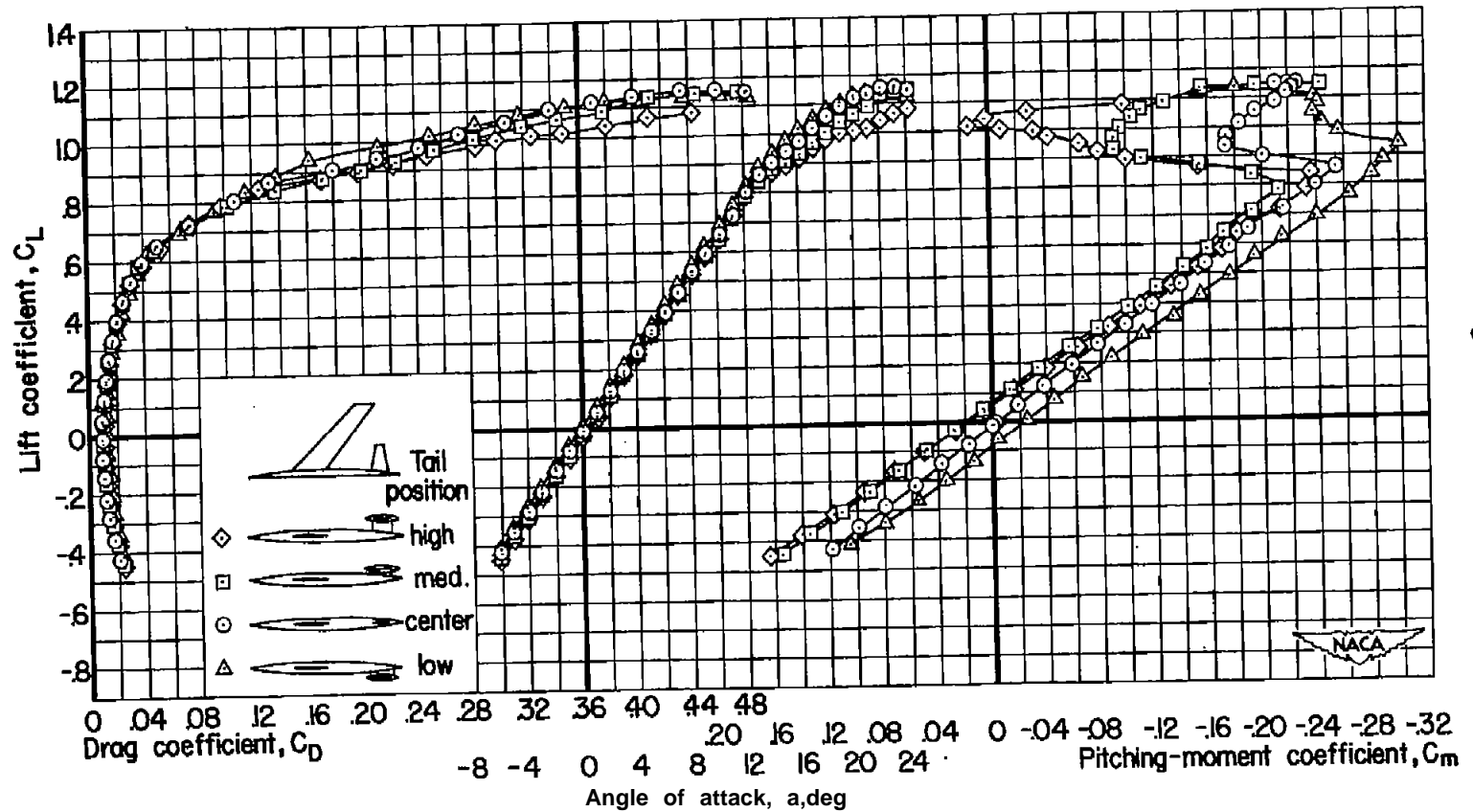
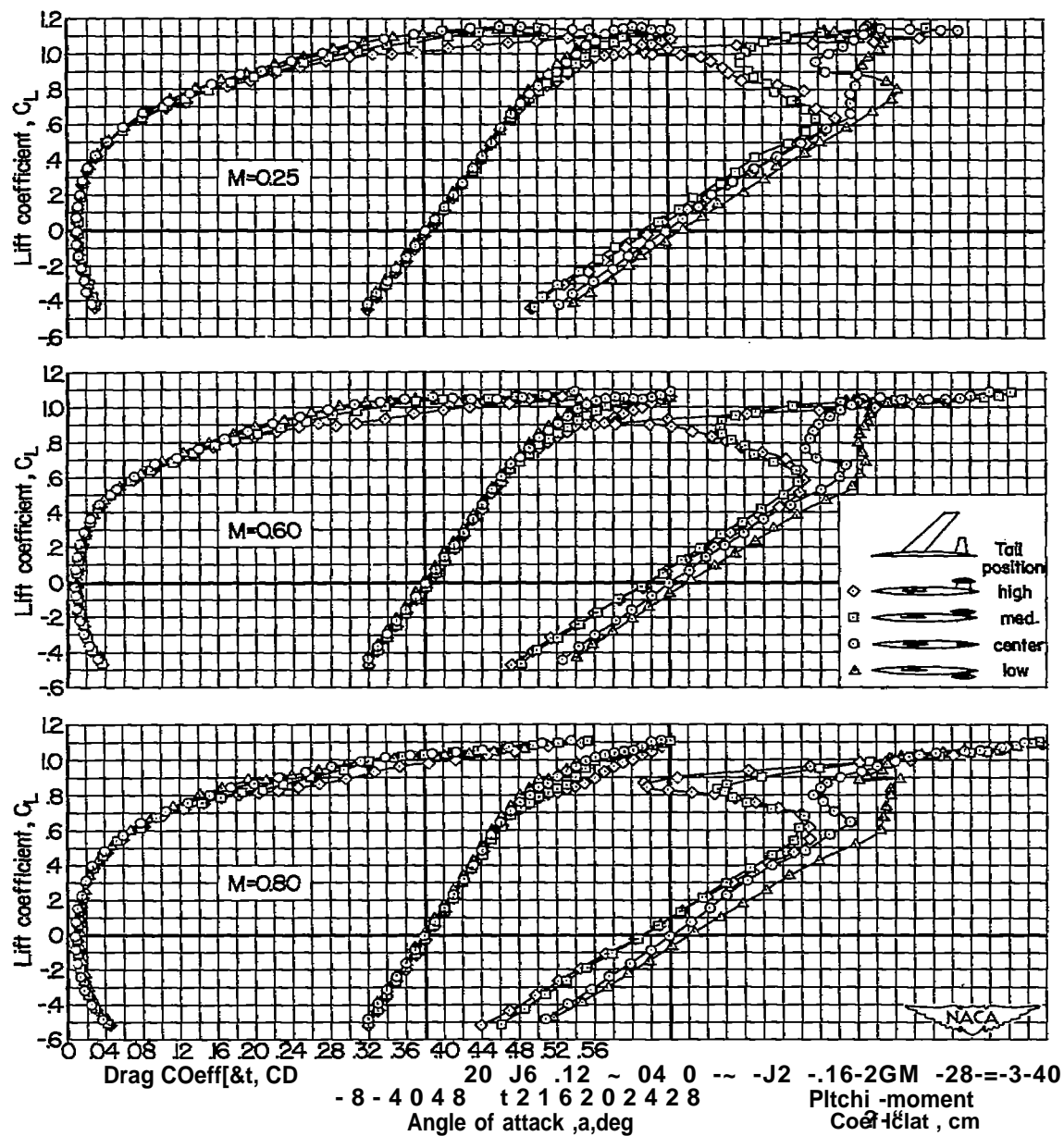


Figure 5. - The effect of tail height on the aerodynamic characteristics of the del at a Reynolds number of 10,000,000; $\alpha = 0^\circ$.



(a) $M = 0.25, 0.60, \text{ and } 0.80$.

Figure 6.- The effect of tail height on the aerodynamic characteristics of the model at various Mach numbers; $R = 2,000,000$.

CONFIDENTIAL

NACA RM A54K09

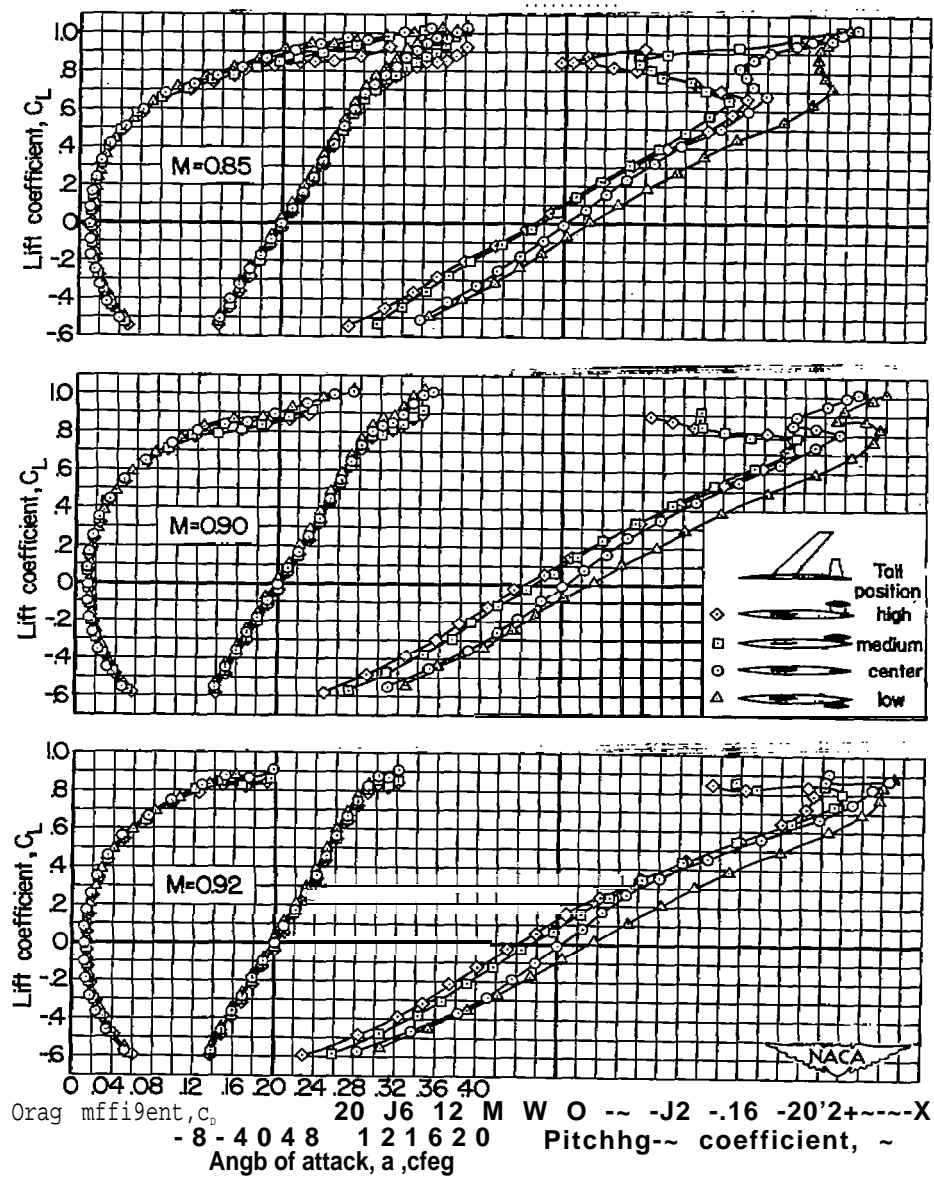
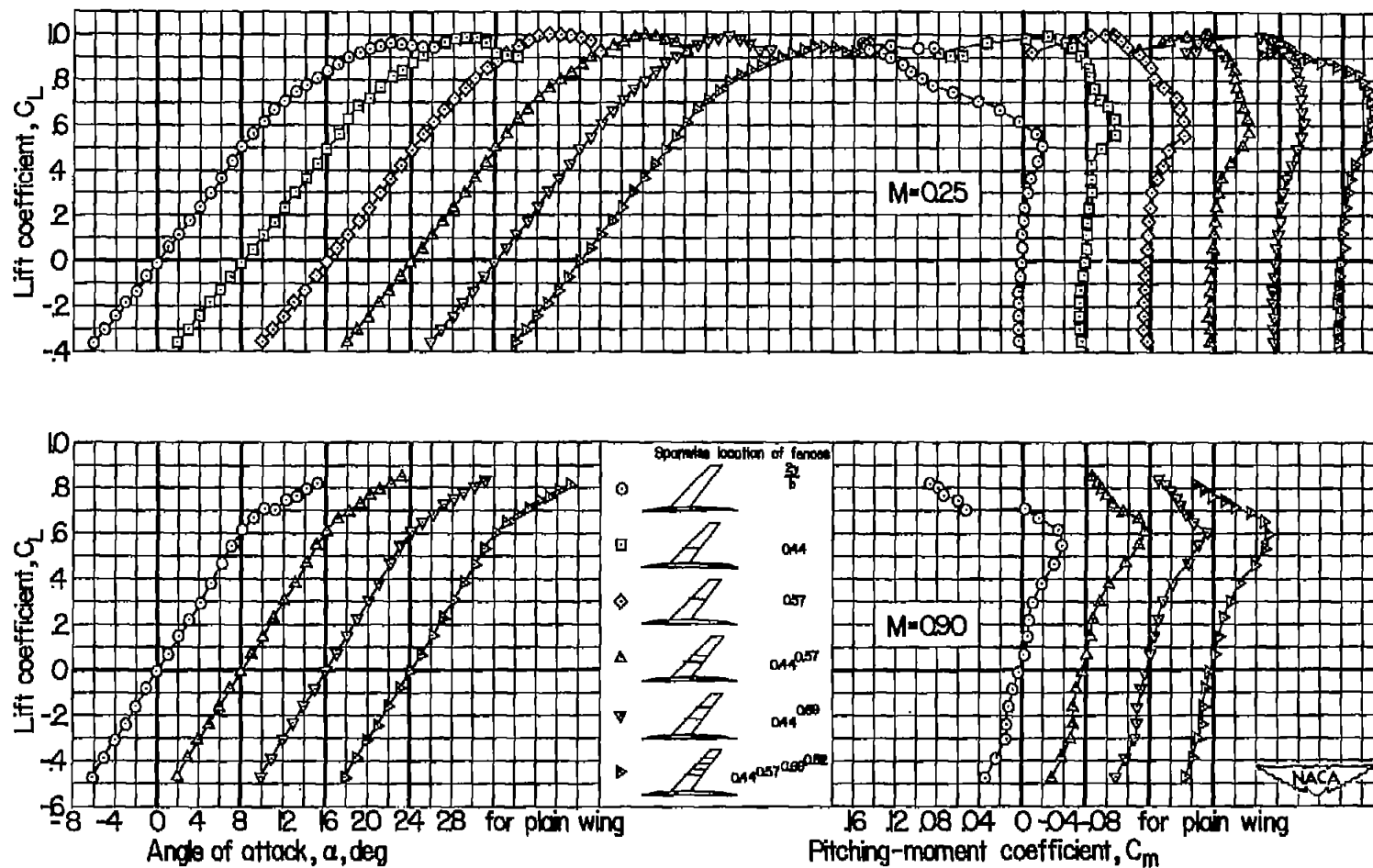
(b) $M = 0.85, 0.90, \text{ and } 0.92$.

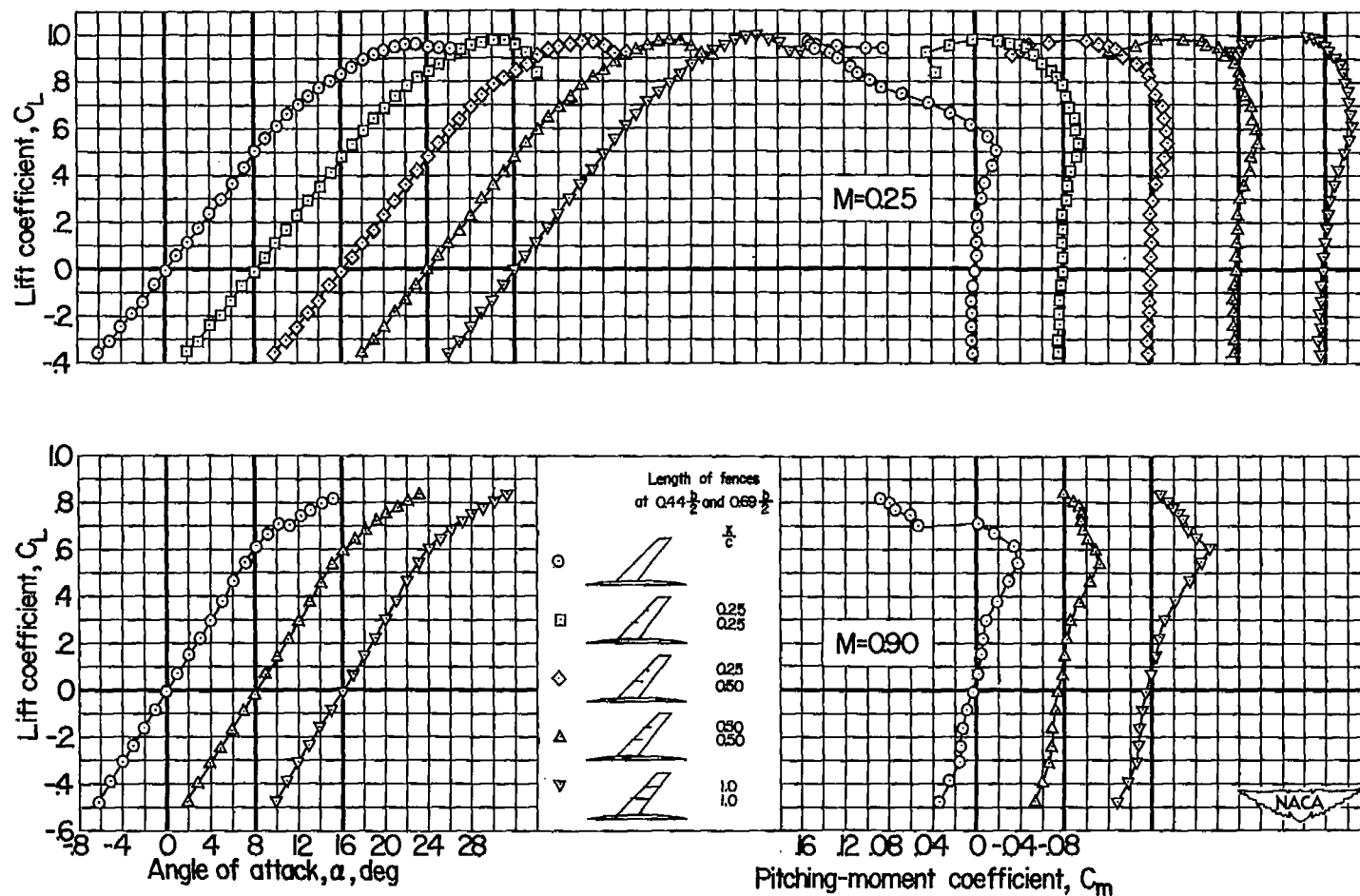
Figure 6.- Concluded.

CONFIDENTIAL



(a) Effect of Span location.

Figure 7.- Lift and pitching-moment characteristics of the model with tie tail off and with various combinations of fences at Mach numbers of 0.25 and 0.90; $R = 2,000,000$.



(b) Effect of fence length.

Figure 7.- Concluded.

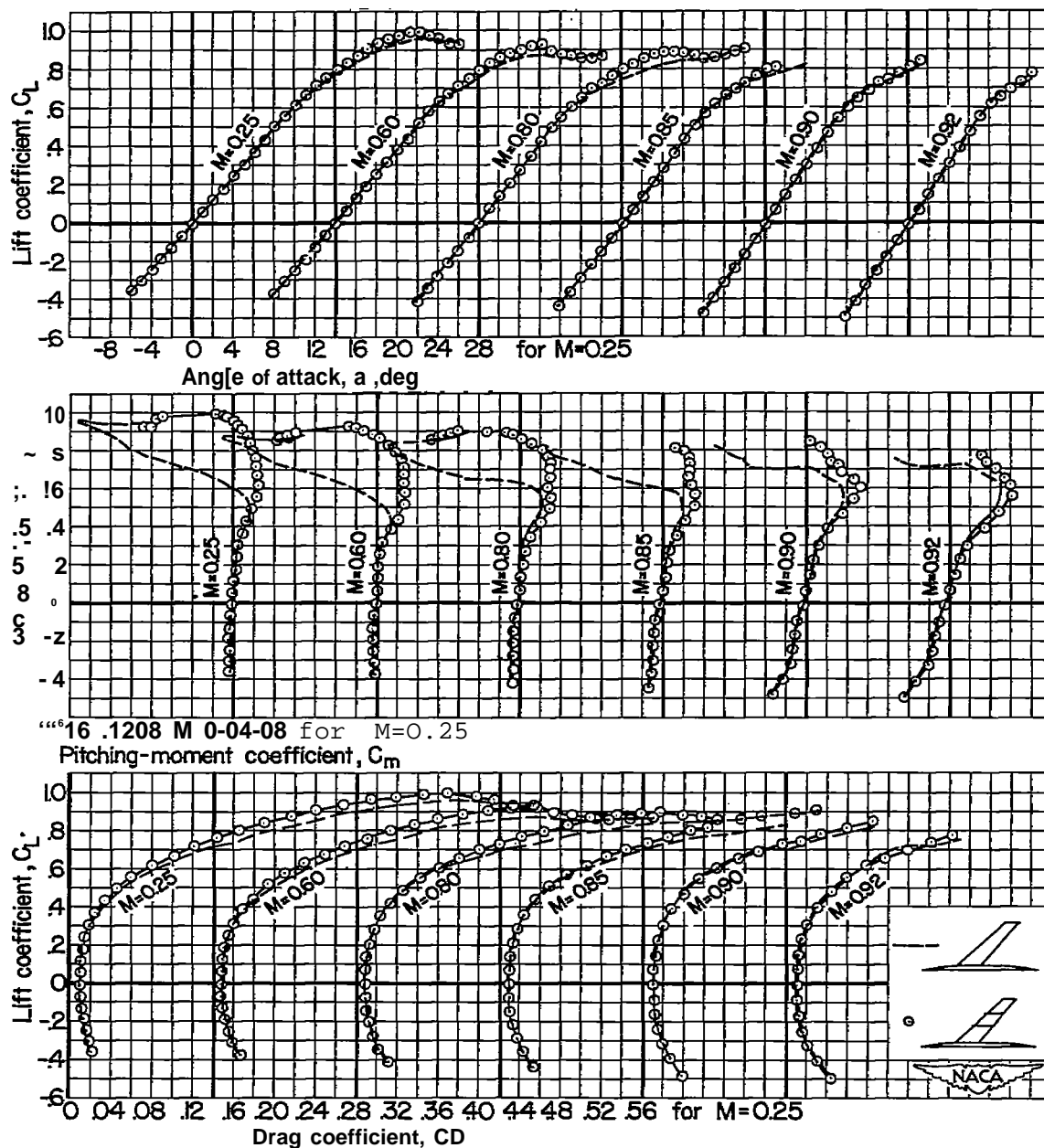


Figure 8.- aerodynamic characteristics of the rafter with the tail off at various Mach numbers; $R = 2,000,000$.

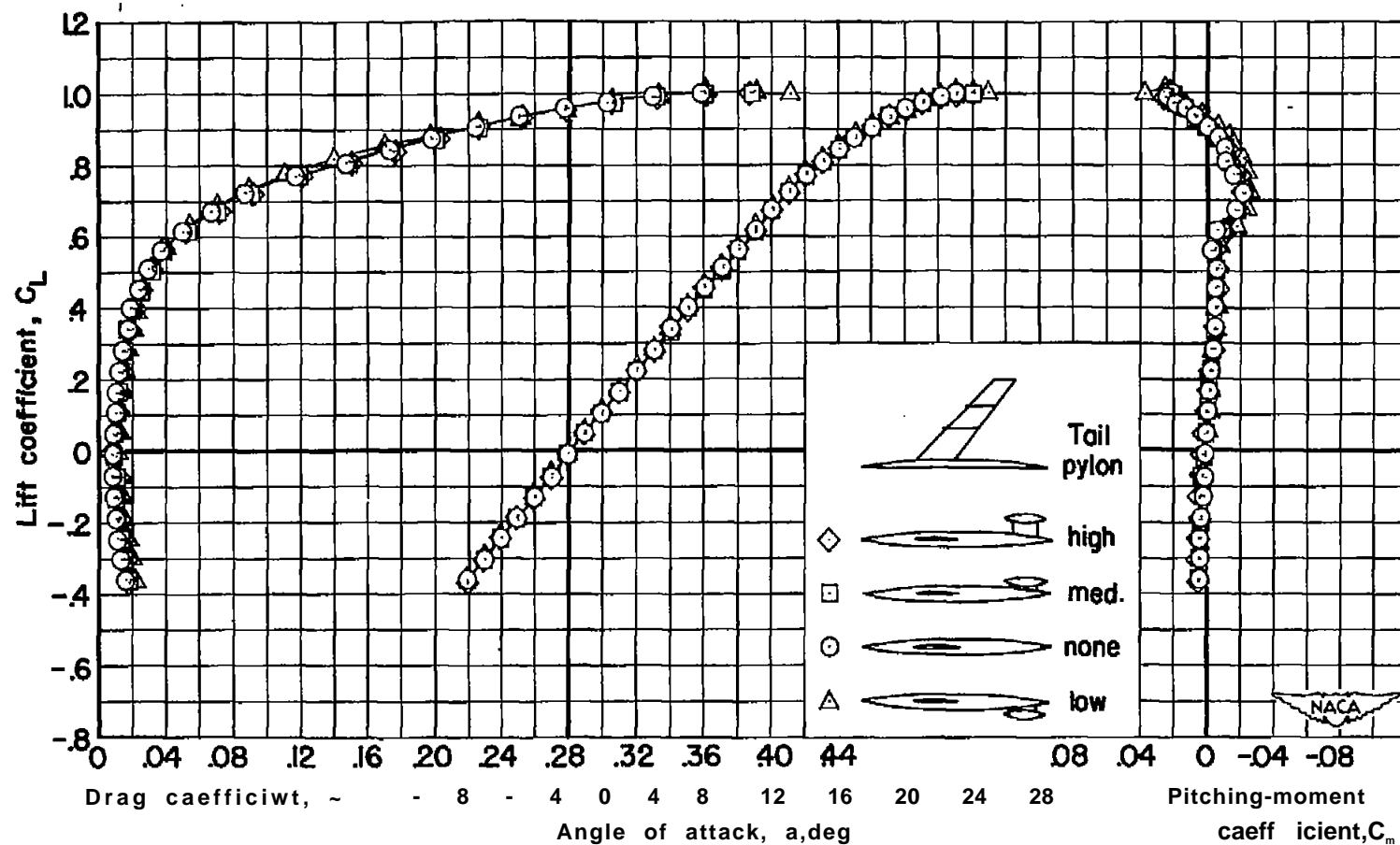


Figure 9.- The aerodynamic characteristics of the model with fences at 0. U and 0.69 semispan, G_{il} off, and with various tail support pylons at a Reynolds number of 10,000; $M = 0.5$.

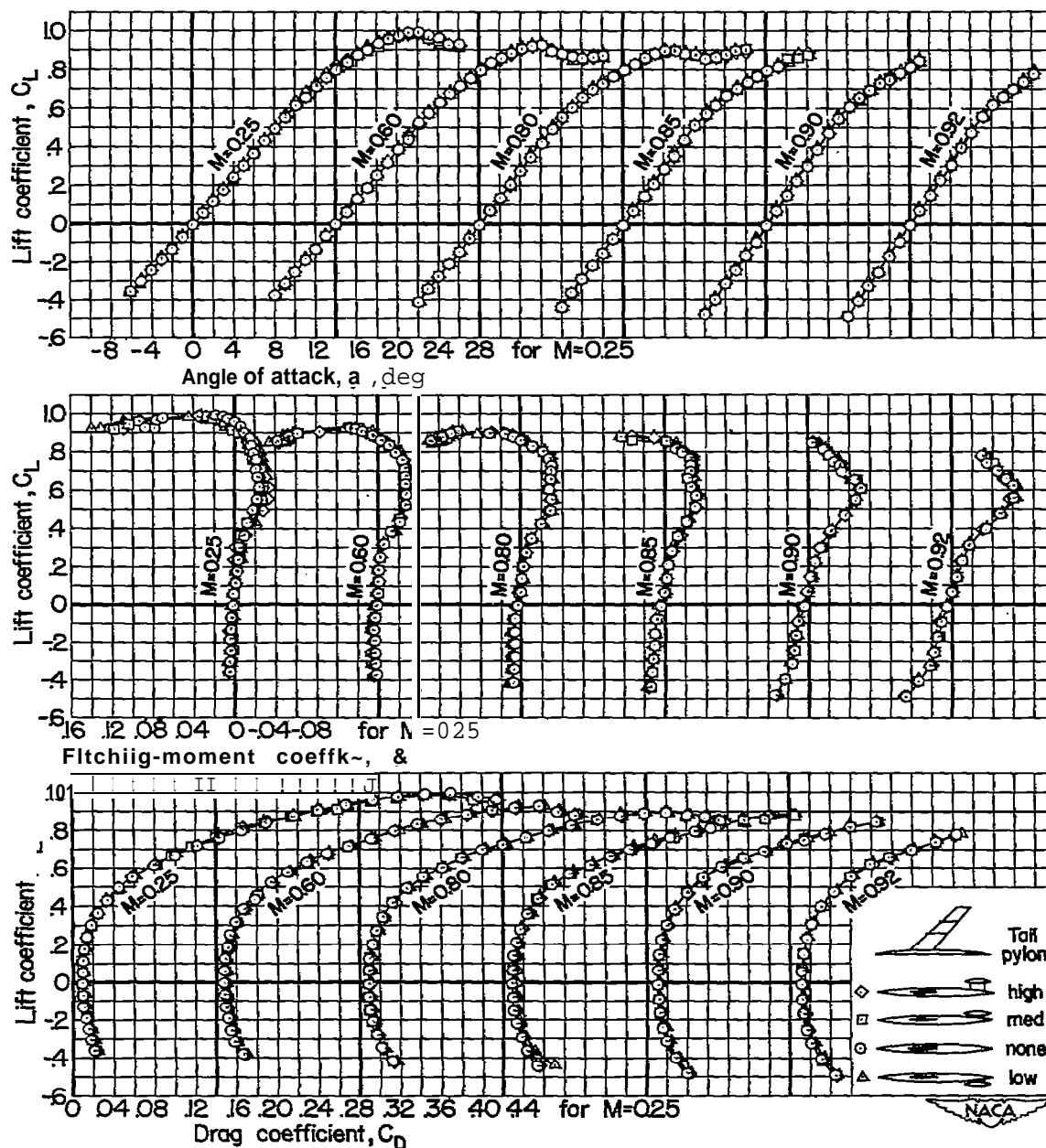
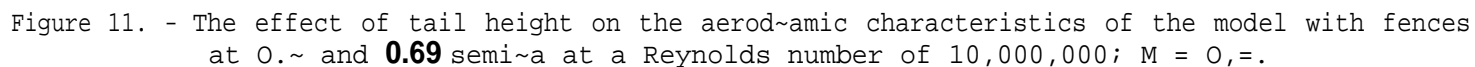
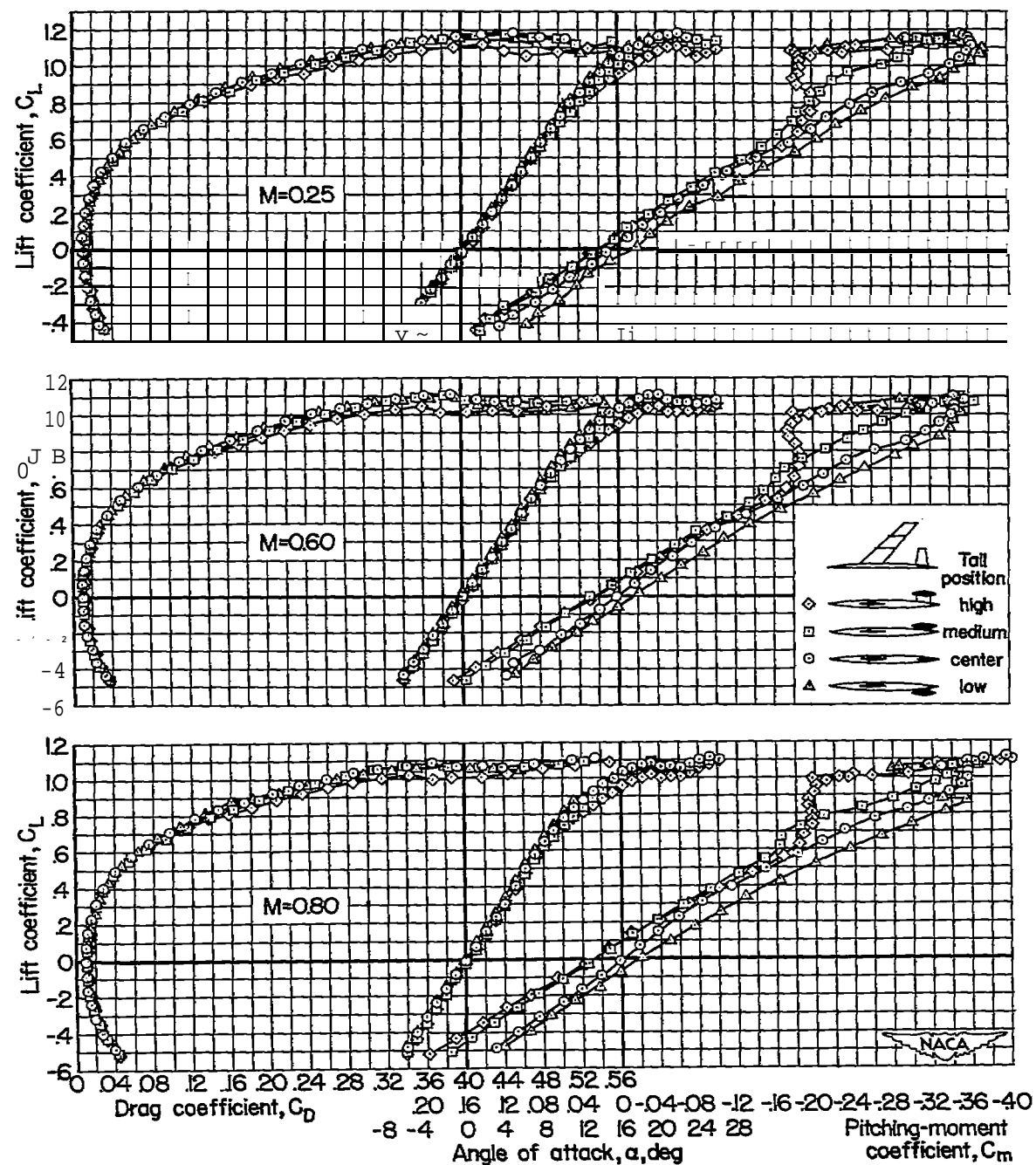


Figure 10. - The aerodynamic characteristics of the model with fences at 0.44 and 0.69 span, tail off, and with various tail support pylons at several Mach numbers; $R = 2,000,000$.





(a) $\sim = 0.25, 0.\sim,$ and 0.80 .

Figure 12. - The effect of tail height on the aerodynamic characteristics of the model with fences at 0.44 and 0.69 semichord at various Mach numbers; $R = 2,000$ y--

CONFIDENTIAL

NACA RM A54K09

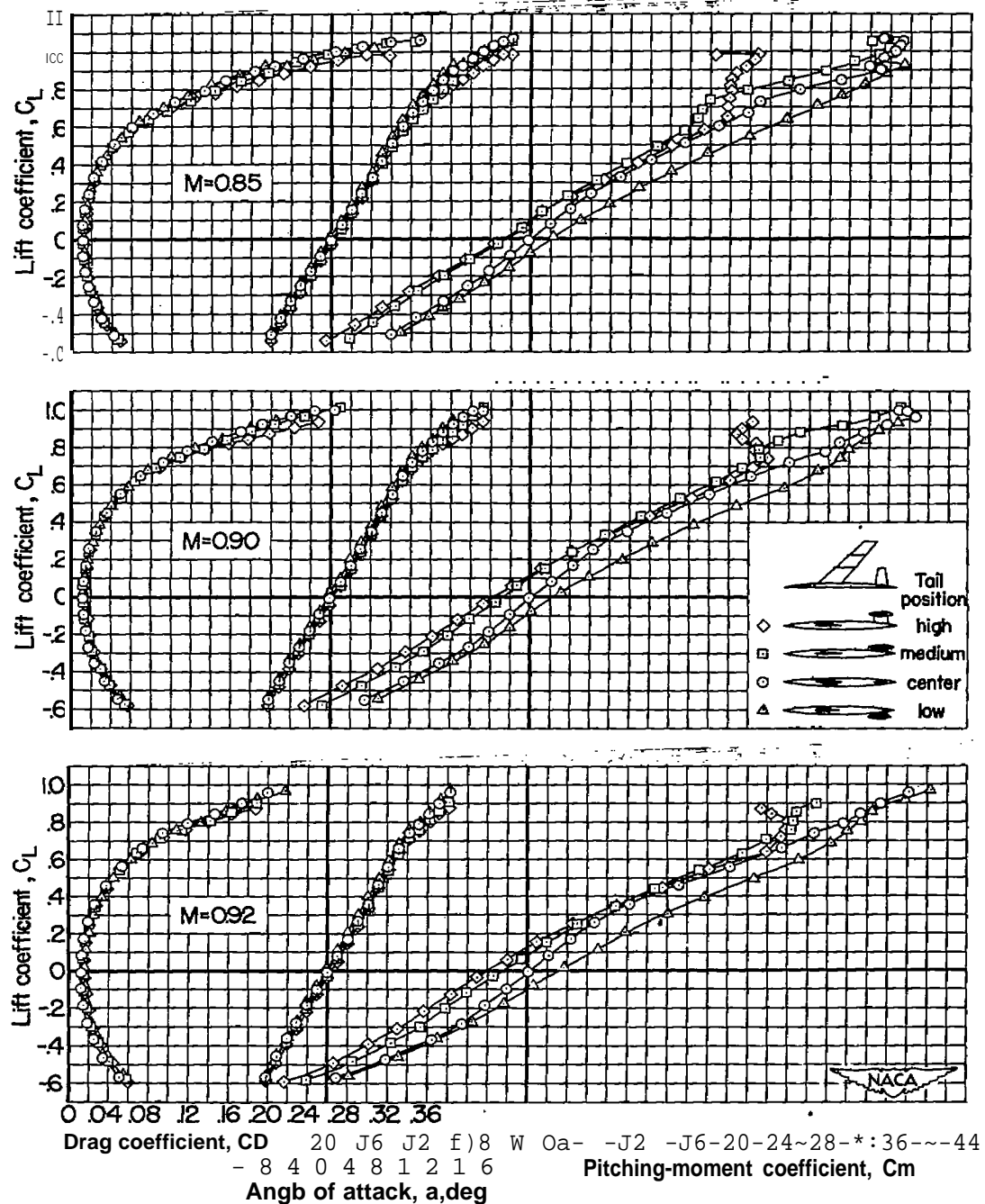
(b) $M = 0.85, 0.90$, and 0.92 .

Figure 12. - Concluded.

CONFIDENTIAL

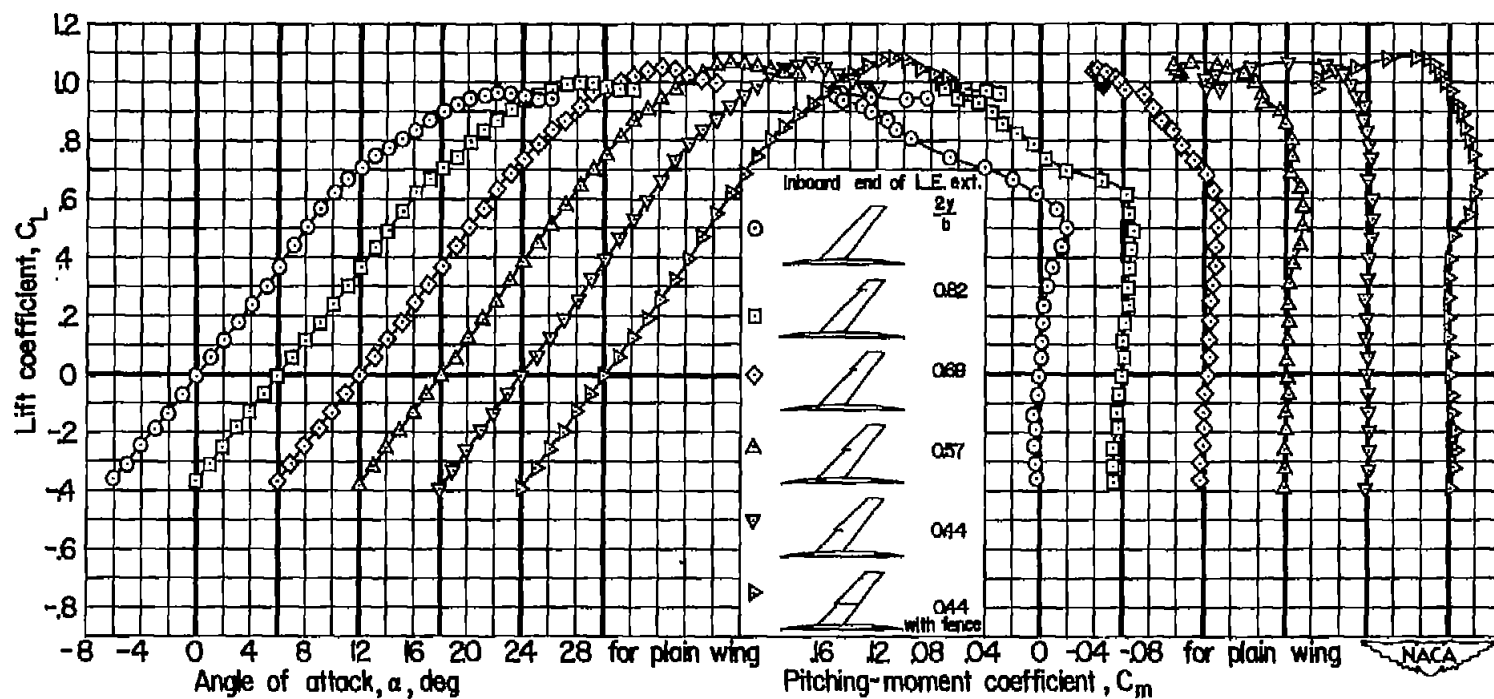


Figure 13. - Lift and pitching-moment characteristics of the model with the tail off and with various leading-edge extension and leading-edge extension-fence combination at a Mach number of 0.3; $Re = 2,000$, (XKI).

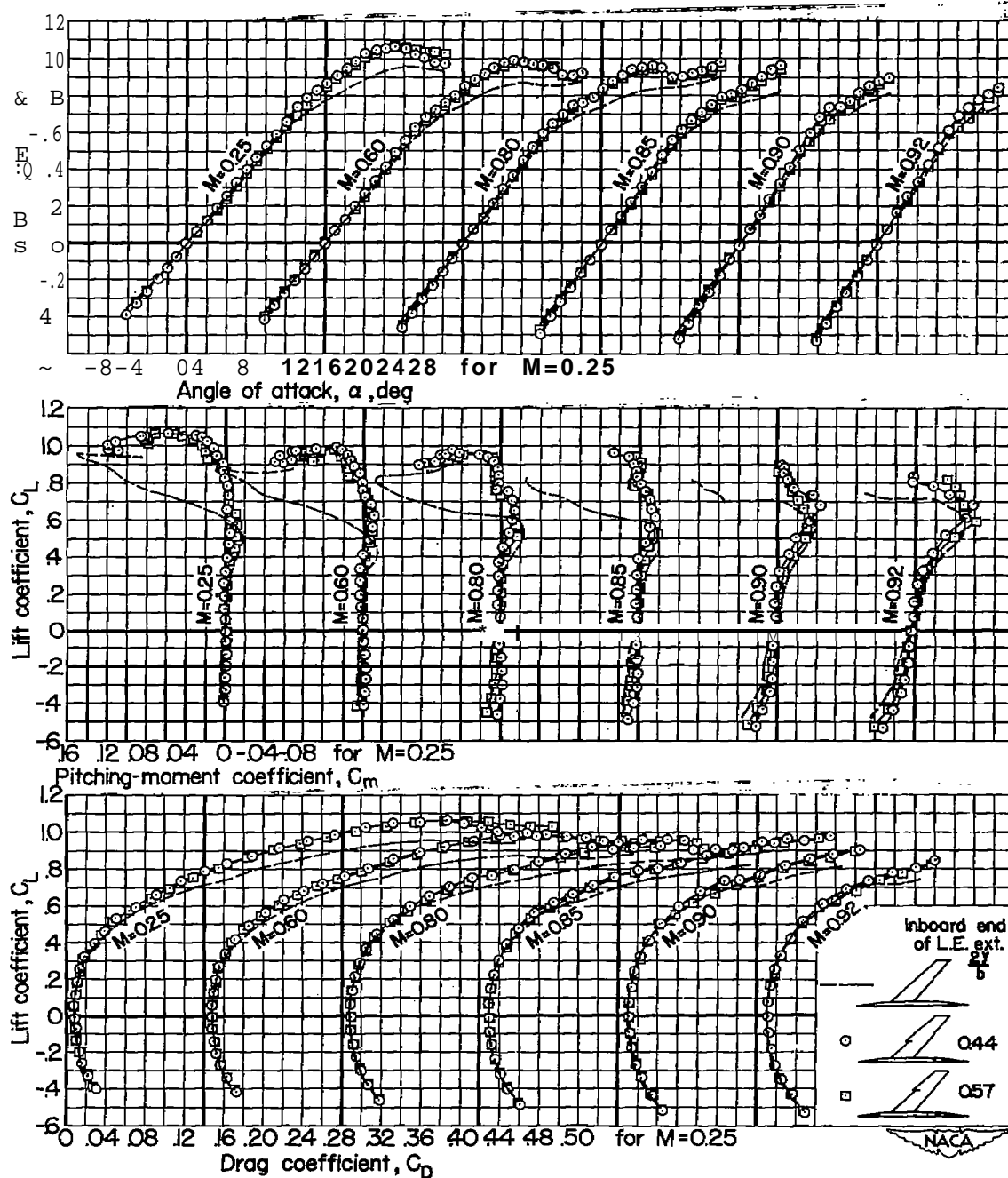


Figure 14. - The effect of leading-edge extensions on the aerodynamic characteristics of the model with tail off at various Mach numbers.

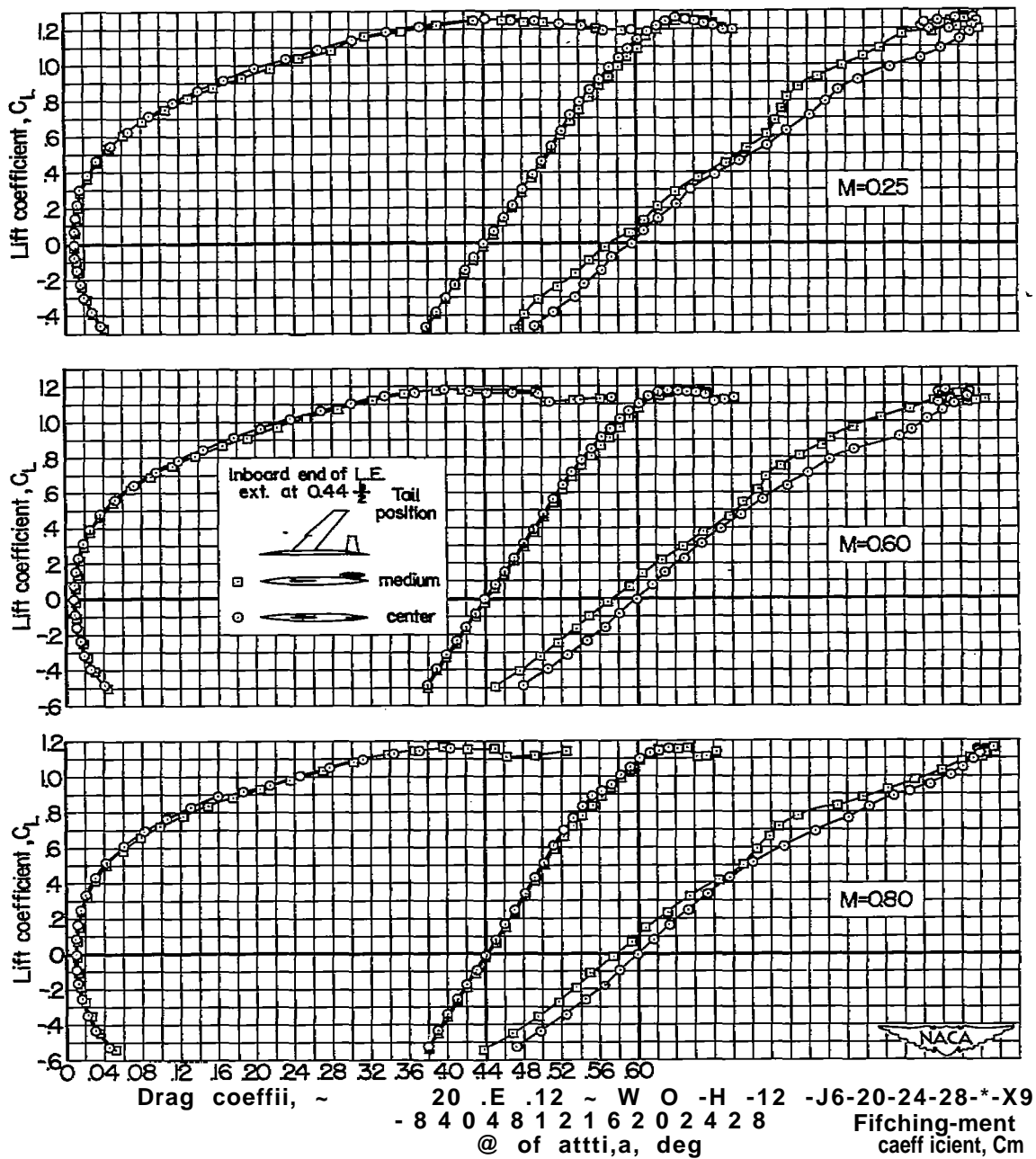
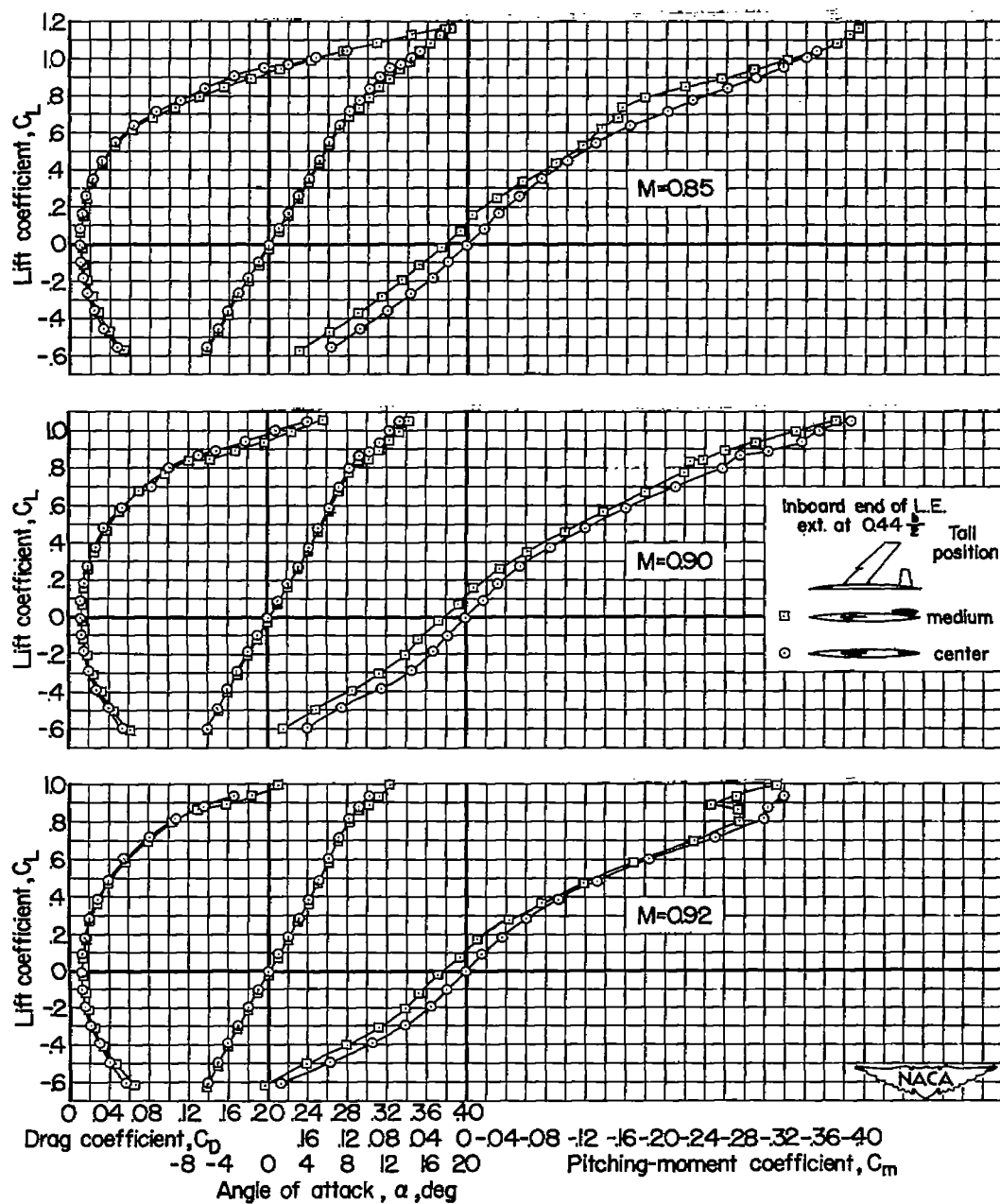
(a) $M = 0.25, 0.60, \text{ and } 0.80$.

Figure 15. - the effect of tail height on the model with a leading-edge extension between the tip and 0.5 semi span at various Mach numbers; $R = 2, 4, 8, 16, 32, 64, 128, 256, 512, 1024, 2048, 4096, 8192, 16384, 32768, 65536, 131072, 262144, 524288, 1048576, 2097152, 4194304, 8388608, 16777216, 33554432, 67108864, 134217728, 268435456, 536870912, 1073741824, 2147483648, 4294967296, 8589934592, 17179869184, 34359738368, 68719476736, 137438953472, 274877906944, 549755813888, 1099511627776, 2199023255552, 4398046511104, 8796093022208, 17592186044416, 35184372088832, 70368744177664, 140737488355328, 281474976710656, 562949953421312, 1125899906842624, 2251799813685248, 4503599627370496, 9007199254740992, 18014398509481984, 36028797018963968, 72057594037927936, 144115188075855872, 288230376151711744, 576460752303423488, 1152921504606846976, 2305843009213693952, 4611686018427387904, 9223372036854775808, 18446744073709551616, 36893488147419103232, 73786976294838206464, 147573952589676412928, 295147905179352825856, 590295810358705651712, 1180591620717411303424, 2361183241434822606848, 4722366482869645213696, 9444732965739290427392, 18889465931478580854784, 37778931862957161709568, 75557863725914323419136, 151115727451828646838272, 302231454903657293676544, 604462909807314587353088, 1208925819614629174706176, 2417851639229258349412352, 4835703278458516698824704, 9671406556917033397649408, 19342813113834066795298816, 38685626227668133590597632, 77371252455336267181195264, 154742504910672534362390528, 309485009821345068724781056, 618970019642690137449562112, 1237940039285380274899124224, 2475880078570760549798248448, 4951760157141521099596496896, 9903520314283042199192993792, 19807040628566084398385987584, 39614081257132168796771975168, 79228162514264337593543950336, 158456325028528675187087900672, 316912650057057350374175801344, 633825300114114700748351602688, 1267650600228229401496703205376, 2535301200456458802993406410752, 5070602400912917605986812821504, 10141204801825835211973625643008, 20282409603651670423947251286016, 40564819207303340847894502572032, 81129638414606681695789005144064, 162259276829213363391578010288128, 324518553658426726783156020576256, 649037107316853453566312041152512, 1298074214633706907132624082305024, 2596148429267413814265248164610048, 5192296858534827628530496329220096, 10384593717069655257060992658440192, 20769187434139310514121985316880384, 41538374868278621028243970633760768, 83076749736557242056487941267521536, 166153499473114484112975882535043072, 332306998946228968225951765070086144, 664613997892457936451903530140172288, 1329227995784915872903807060280344576, 2658455991569831745807614120560689152, 5316911983139663491615228241121378304, 10633823966279326983230456482242756608, 21267647932558653966460912964485513216, 42535295865117307932921825928971026432, 85070591730234615865843651857942052864, 170141183460469231731687303715884105728, 340282366920938463463374607431768211456, 680564733841876926926749214863536422912, 1361129467683753853853498429727072845824, 2722258935367507707706996859454145691648, 5444517870735015415413993718908291383296, 10889035741470030830827987437816582766592, 21778071482940061661655974875633165533184, 43556142965880123323311949751266331066368, 87112285931760246646623899502532662132736, 174224571863520493293247799005065324265472, 348449143727040986586495598010130648530944, 696898287454081973172991196020261297061888, 1393796574908163946345982392040522594123776, 2787593149816327892691964784081045188247552, 5575186299632655785383929568162090376495104, 11150372599265311570767859136324180752990208, 22300745198530623141535718272648361505980416, 44601490397061246283071436545296723011960832, 89202980794122492566142873090593446023921664, 178405961588244985132285746181186892047843328, 356811923176489970264571492362373784095686656, 713623846352979940529142984724747568191373312, 1427247692705959881058285969449495136382746624, 2854495385411919762116571938898990272765493248, 5708990770823839524233143877797980545530986496, 11417981541647679048466287755595961091061972992, 22835963083295358096932575511191922182123945984, 45671926166590716193865151022383844364247891968, 91343852333181432387730302044767688728495783936, 182687704666362864775460604089535377456991567872, 365375409332725729550921208179070754913983135744, 730750818665451459101842416358141509827966271488, 1461501637330902918203684832716283019655932542976, 2923003274661805836407369665432566039311865085952, 5846006549323611672814739330865132078623730171904, 11692013098647223345629478661730264157247460343808, 23384026197294446691258957323460528314494920687616, 46768052394588893382517914646921056628989841375232, 93536104789177786765035829293842113257979682750464, 187072209578355573530071658587684226515959365500928, 374144419156711147060143317175368453031918731001856, 748288838313422294120286634350736906063837462003712, 1496577676626844588240573268701473812127674924007424, 2993155353253689176481146537402947624255349848014848, 5986310706507378352962293074805895248510699696029696, 11972621413014756705924586149611790497021399392059392, 23945242826029513411849172299223580994042798784118784, 47890485652059026823698344598447161988085597568237568, 95780971304118053647396689196894323976171195136475136, 191561942608236107294793378393788647952342390272950272, 383123885216472214589586756787577295904684780545900544, 766247770432944429179173513575154591809369561091801088, 1532495540865888858358347027150309183618739122183602176, 3064991081731777716716694054300618367237478244367204352, 6129982163463555433433388108601236734474956488734408704, 12259964326927110866866776217202473468949912977468817408, 24519928653854221733733552434404946937899825954937634816, 49039857307708443467467104868809893875799651909875269632, 98079714615416886934934209737619787751599303819750539264, 196159429230833773869868419475239575503198607639501078528, 392318858461667547739736838950479151006397215279002157056, 784637716923335095479473677900958302012794430558004314112, 1569275433846670190958947355801916604025588861116008628224, 3138550867693340381917894711603833208051177722232017256448, 6277101735386680763835789423207666416102355444464034512896, 12554203470773361527671578846415332832204710888928069025792, 25108406941546723055343157692830665664409421777856138051584, 50216813883093446110686315385661331328818843555712276103168, 100433627766186892221372630771322662657637687111424552206336, 200867255532373784442745261542645325315275374222849104412672, 401734511064747568885490523085290650630550748445698208825344, 803469022129495137770981046170581301261101496891396417650688, 1606938044258990275541962092341162602522202993782792835301376, 3213876088517980551083924184682325205044405987565585670602752, 6427752177035961102167848369364650410088811975131171341205504, 12855504354071922204335696738729300820177623950262342682411008, 25711008708143844408671393477458601640355247900524685364822016, 51422017416287688817342786954917203280710495801049370729644032, 102844034832575377634685573909834406561420991602098741459288064, 205688069665150755269371147819668813122841983204197482918576128, 411376139330301510538742295639337626245683966408394965837152256, 822752278660603021077484591278675252491367932816789931674304512, 1645504557321206042154969182557350504982735865633579863348609024, 3291009114642412084309938365114701009965471731267159726697218048, 6582018229284824168619876730229402019930943462534319453394436096, 13164036458569648337239753460458804039861886925068638906788872192, 26328072917139296674479506920917608079723773850137277813577744384, 52656145834278593348959013841835216159447547700274555627155488768, 105312291668557186697918027683670432318895095400549111254310977536, 210624583337114373395836055367340864637790190801098222508621955072, 421249166674228746791672110734681729275580381602196445017243910144, 842498333348457493583344221469363458551160763204392890034487820288, 1684996666696914987166688442938726917102321526408785780068975640576, 3369993333393829974333376885877453834204643052817571560137951281152, 6739986666787659948666753771754907668409286105635143120275902562304, 13479973333575319897333507543509815336818572211270286240551805124608, 26959946667150639794667015087019630673637144422540572481103610249216, 53919893334301279589334030174039261347274288845081144962207220498432, 107839786668602559178668060348078522694548577690162289924414440996864, 215679573337205118357336120696157045389097155380324579848828881993728, 431359146674410236714672241392314090778194310760649159697657763987456, 862718293348820473429344482784628181556388621521298319395315527974912, 1725436586697640946858688965569256363112777243042596638790631055949824, 3450873173395281893717377931138512726225554486085193277581262111899648, 6901746346790563787434755862277025452451108972170386555162524223799296, 13803492693581127574869511724554050904902217944340773110325048447598592, 27606985387162255149739023449108101809804435888681546220650096895197184, 55213970774324510299478046898216203619608871777363092441300193790394368, 110427941548649020598956093796432407239217743554726184882600387580788736, 220855883097298041197912187592864814478435487109452369765200775161577472, 441711766194596082395824375185729628956870974218904739530401550323154944, 883423532389192164791648750371459257913741948437809479060803100646309888, 1766847064778384329583297500742918515827483896875618958121606201292619776, 3533694129556768659166595001485837031654967793751237916243212402585239552, 7067388259113537318333190002971674063309935587502475832486424805170479104, 14134776518227074636666380005943348126619871175004951664972849610340958208, 28269553036454149273332760011886696253239742350009903329945699220681916416, 56539106072908298546665520023773392506479484700019806659891398441363832832, 113078212145816597093331040047546785012958969400039613319782796882727665664, 226156424291633194186662080095093570025917938800079226639565593765455331328, 452312848583266388373324160190187140051835877600158453279131187530910662656, 904625697166532776746648320380374280103671755200316906558262375061821325312, 1809251394333065553493296640760748560207343510400633813116524750123642650624, 3618502788666131106986593281521497120414687020801267626233049500247285301248, 7237005577332262213973186563042994240829374041602535252466099000494570602496, 14474011154664524427946373126085988481658748083205070504932198000989141204992, 28948022309329048855892746252171976963317496166410141009864396001978282409984, 57896044618658097711785492504343953926634992332820282019728792003956564819968, 115792089237316195423570985008687907853269984665640564039457584007913129639936, 231584178474632390847141970017375815706539969331281128078915168015826259279872, 463168356949264781694283940034751631413079938662562256157830336031652518559744, 926336713898529563388567880069503262826159877325124512315660672063305037119488, 1852673427797059126777135760139006525652319754650249024631321344126610074238976, 3705346855594118253554271520278013051304639509300498049262642688253220148477952, 7410693711188236507108543040556026102609279018600996098525285376506440296955904, 14821387422376473014217086081112052205218558037201992197050570753012880593911808, 29642774844752946028434172162224104410437116074403984394101141506025761187823616, 59285549689505892056868344324448208820874232148807968788202283012051522375647232, 118571099379011784113736688648896417641748464297615937576404566024103044751294464, 237142198758023568227473377297792835283496928595231875152809132048206089502588928, 4742843975160471364549467545955856705669938571904637503056182640964121$



(b) $M = 0.85, 0.90, \text{ and } 0.92.$

Figure 15. - Concluded.

CONFIDENTIAL

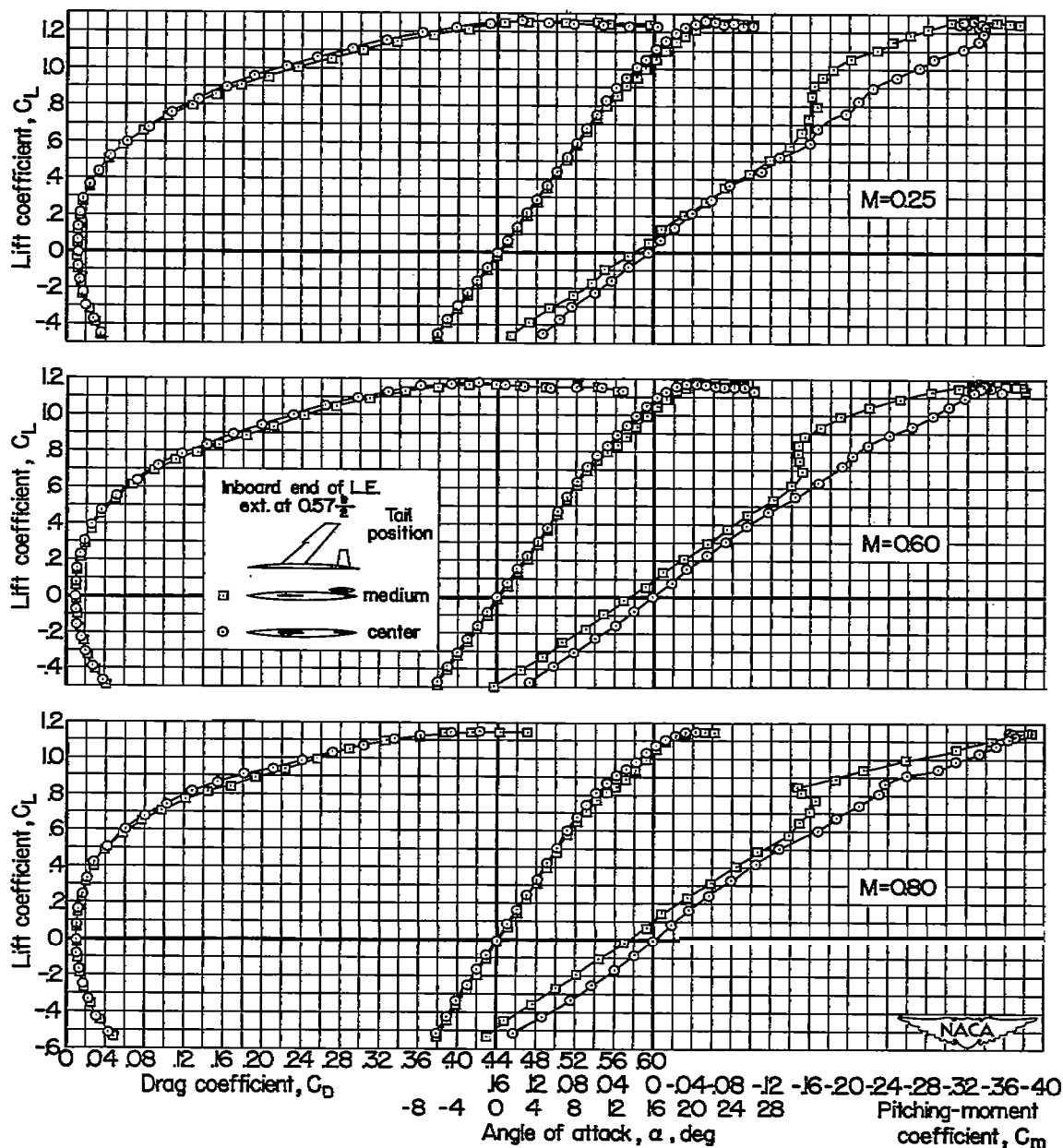
(a) $M = 0.5$, $O.@$, and 0.80 .

Figure 16. - The effect of tail height on the model with a leading-edge extension between the tip and 0.57 semi span at various Mach numbers; $R = 2,000,000$.

CONFIDENTIAL

CONFIDENTIAL

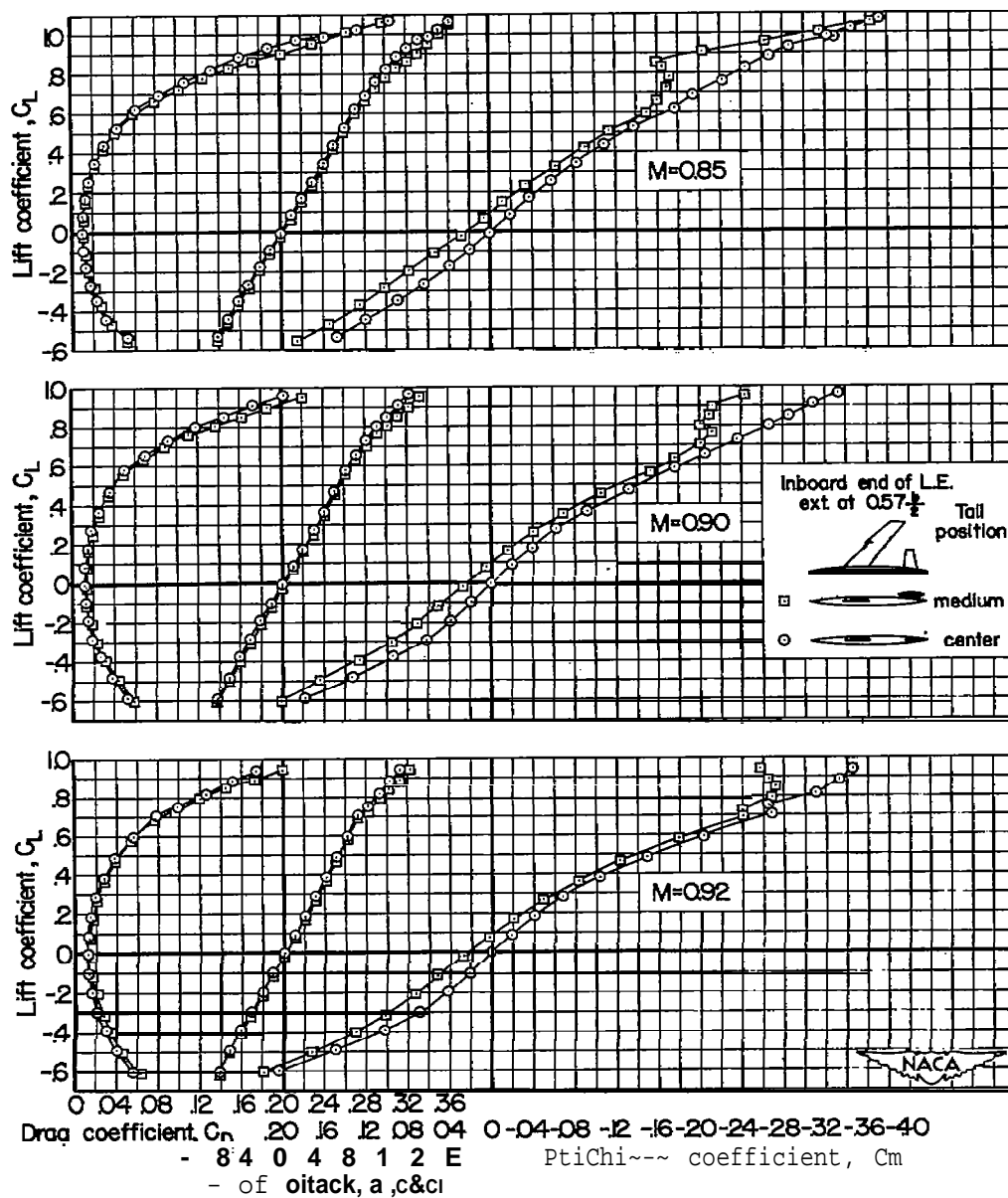
(b) $M = 0.85, 0.90, \text{ and } 0.92$.

Figure 16. - Concluded.

CONFIDENTIAL

CONFIDENTIAL

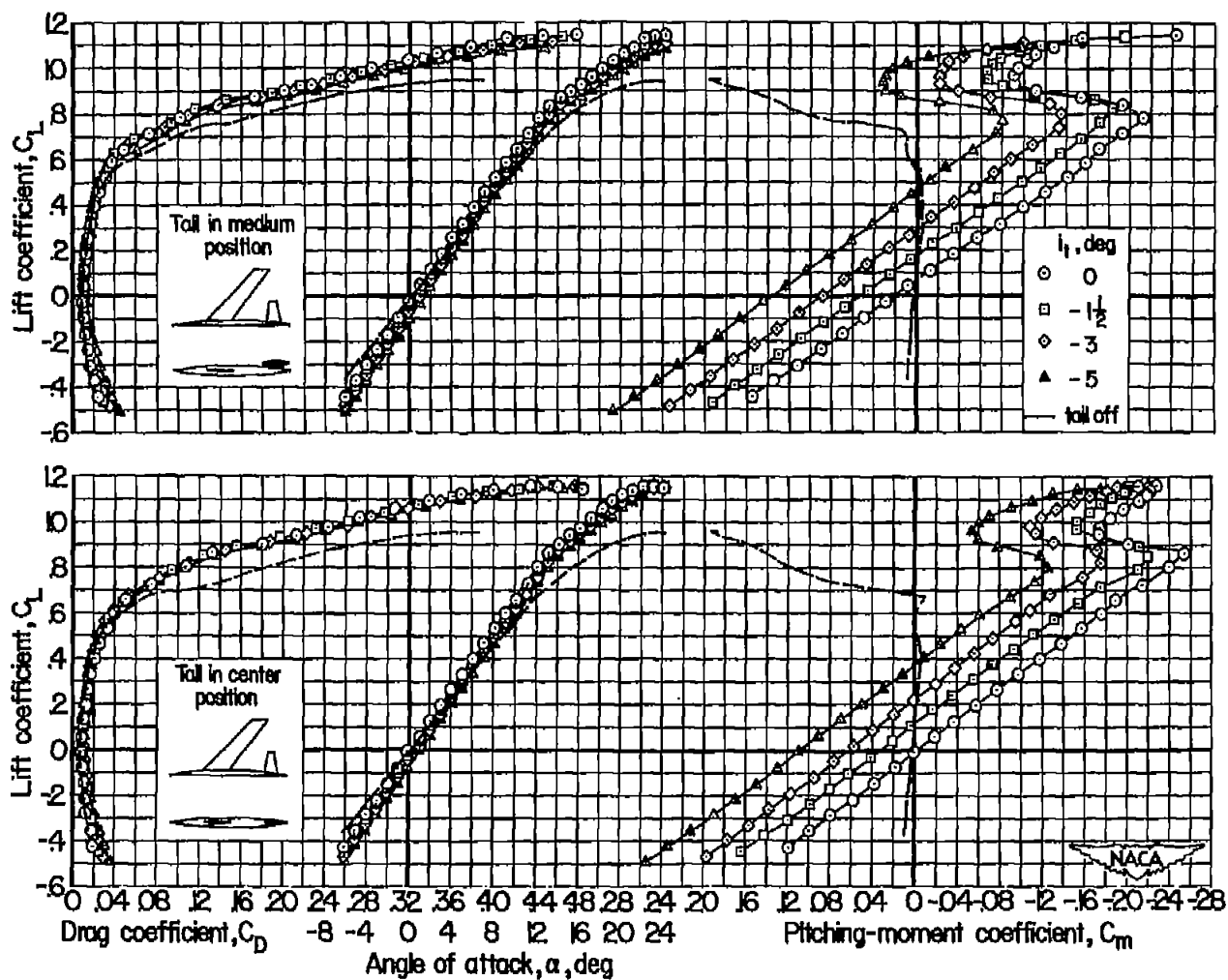
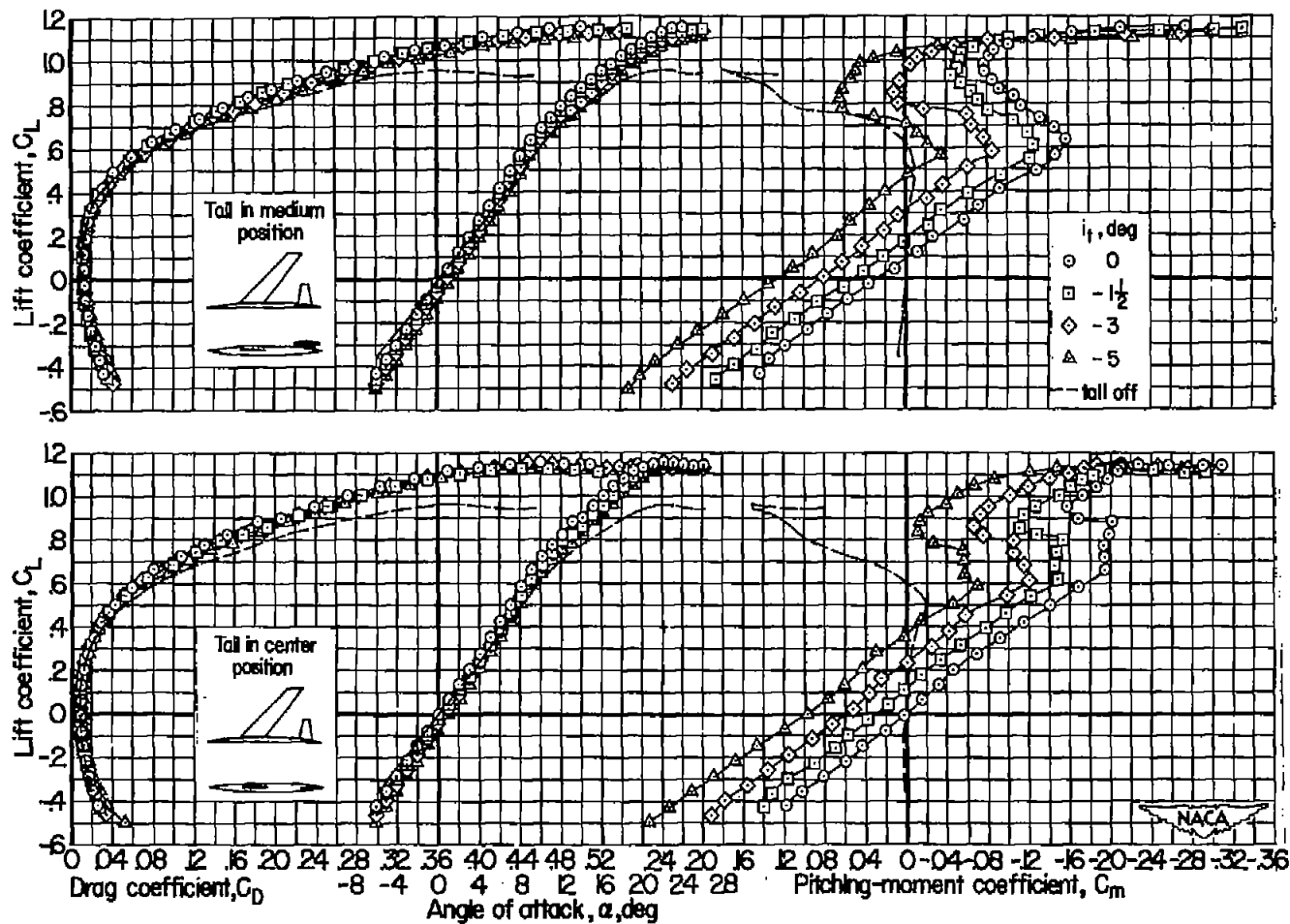


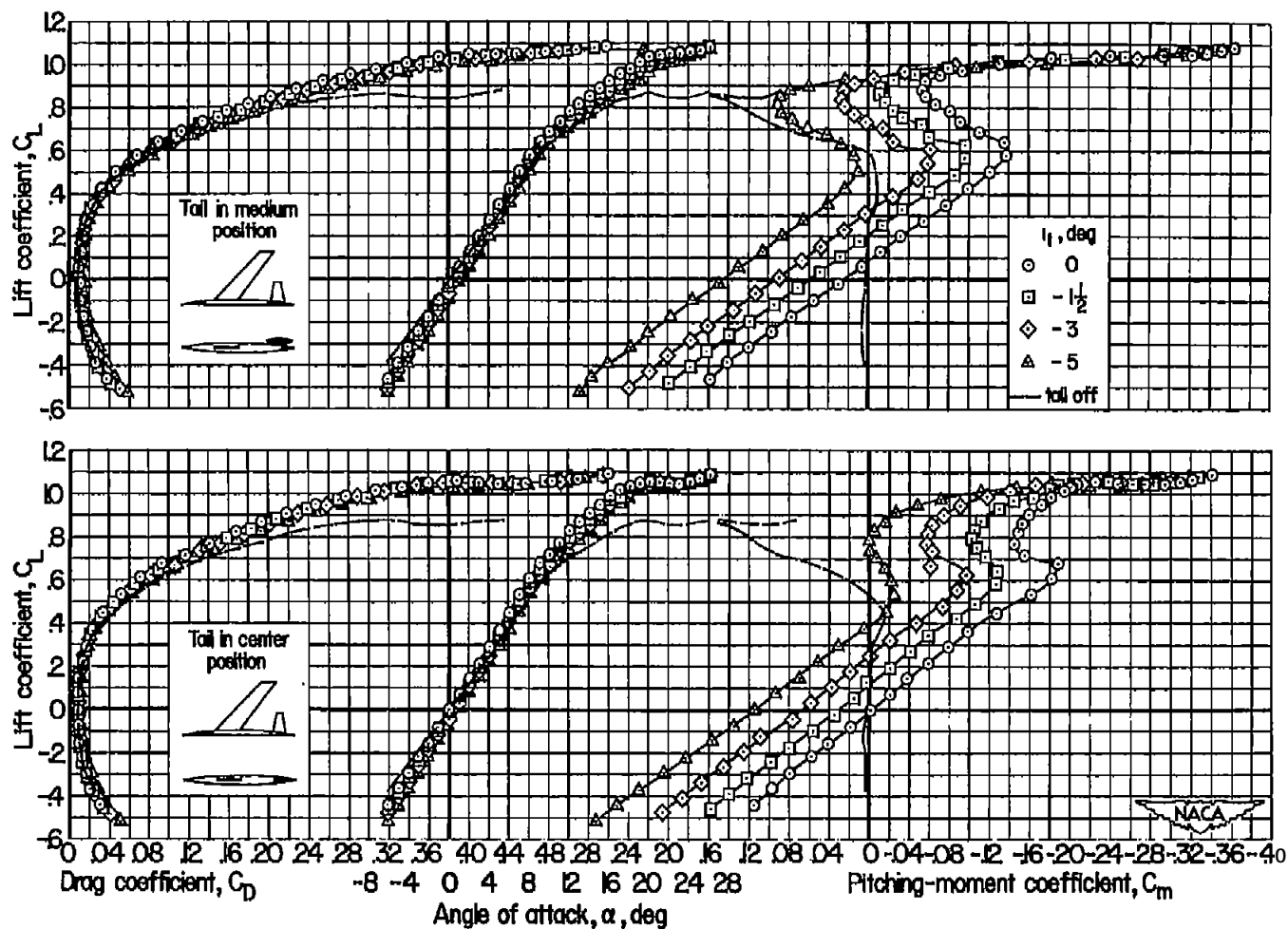
Figure 17. - aerodynamic characteristics of the wing with the tail in the medium and center positions at a Reynolds number of $K, W, W; M = 0.7$.



(a) $M = 0.5$

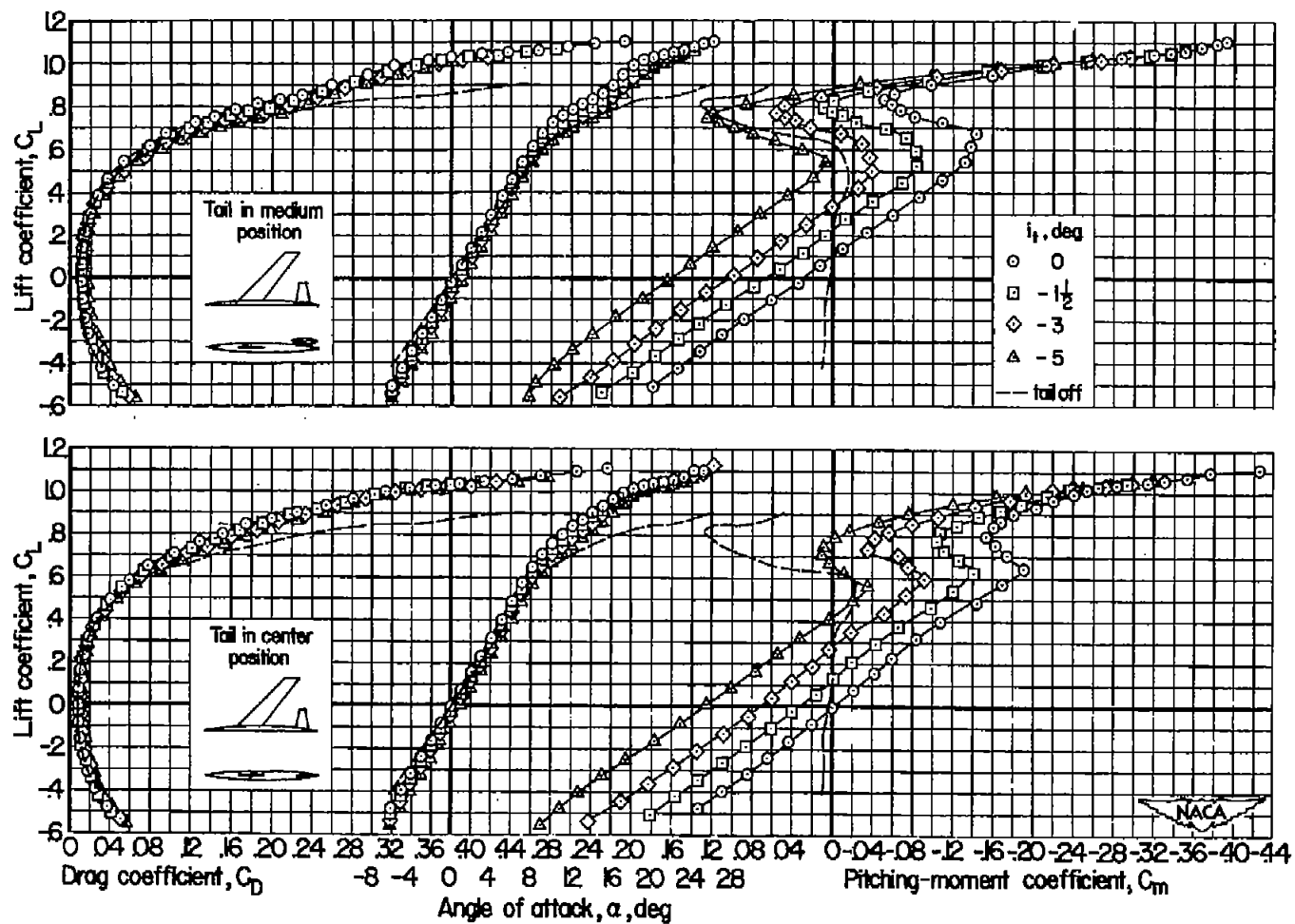
Figure 18. - The aerodynamic characteristics of the model with the M in the medium and center positions at a Reynolds number of 2,000, W_0 .

CONFIDENTIAL



(b) $M = 0.60$

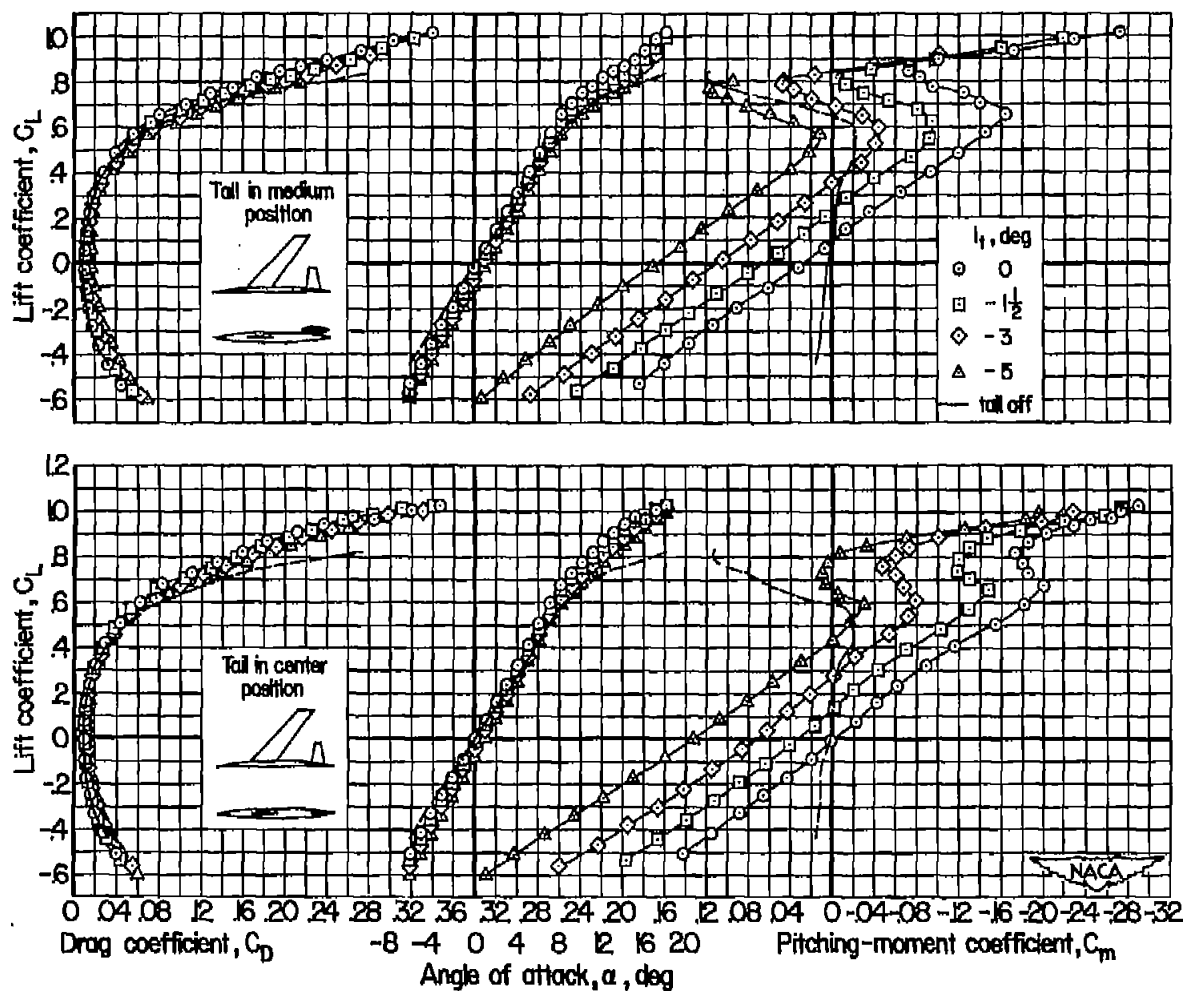
~1~e 18. - Continued.



(c) $M = 0.80$

Figure 13. - Cont~nuea .

CONFIDENTIAL



(d) $M = 0.8\sim$

FTguxc 18. - Continued.

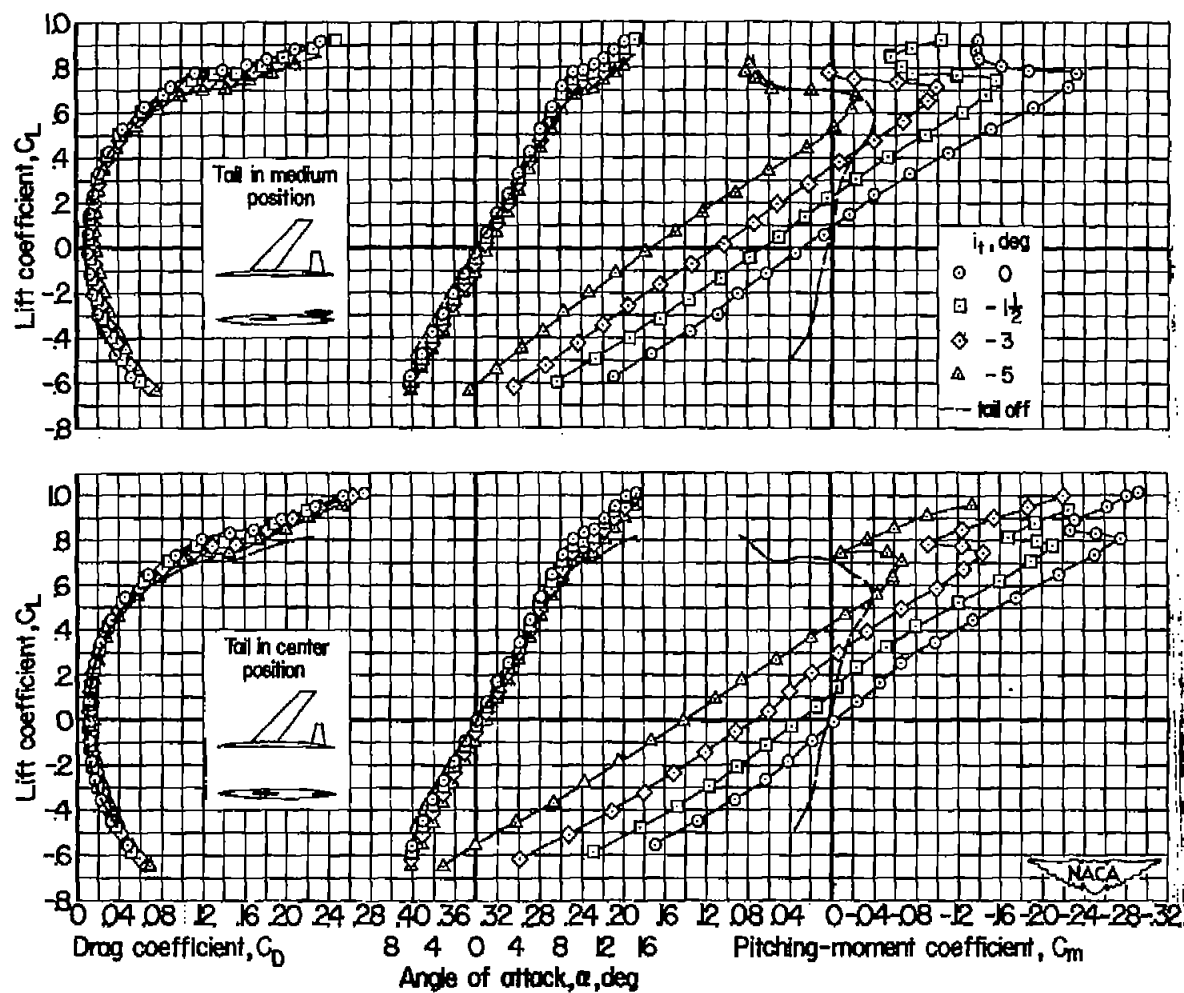
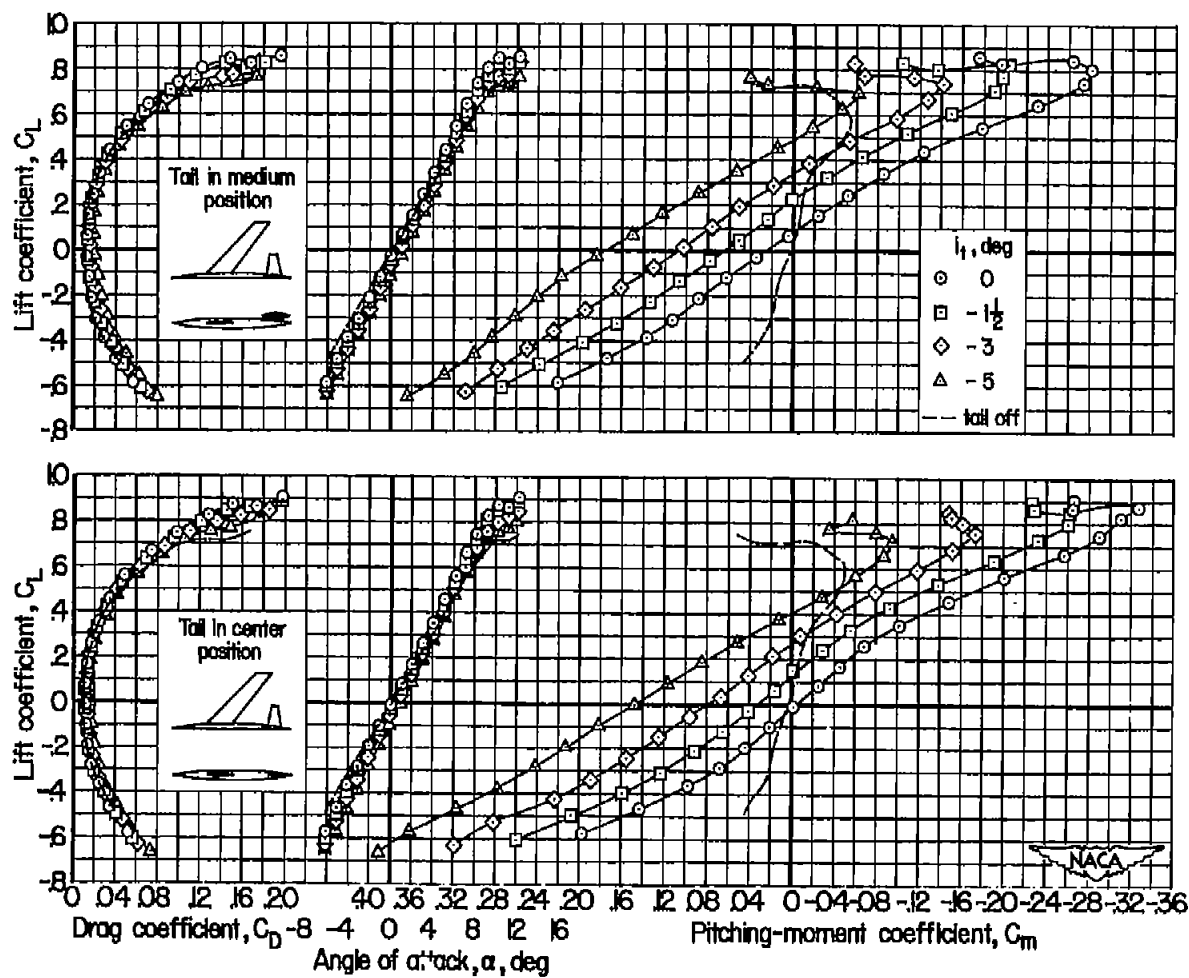
(e) $M = 0.90$

Figure 18. - Continued.



(f) $M = 0.92$

Continued.

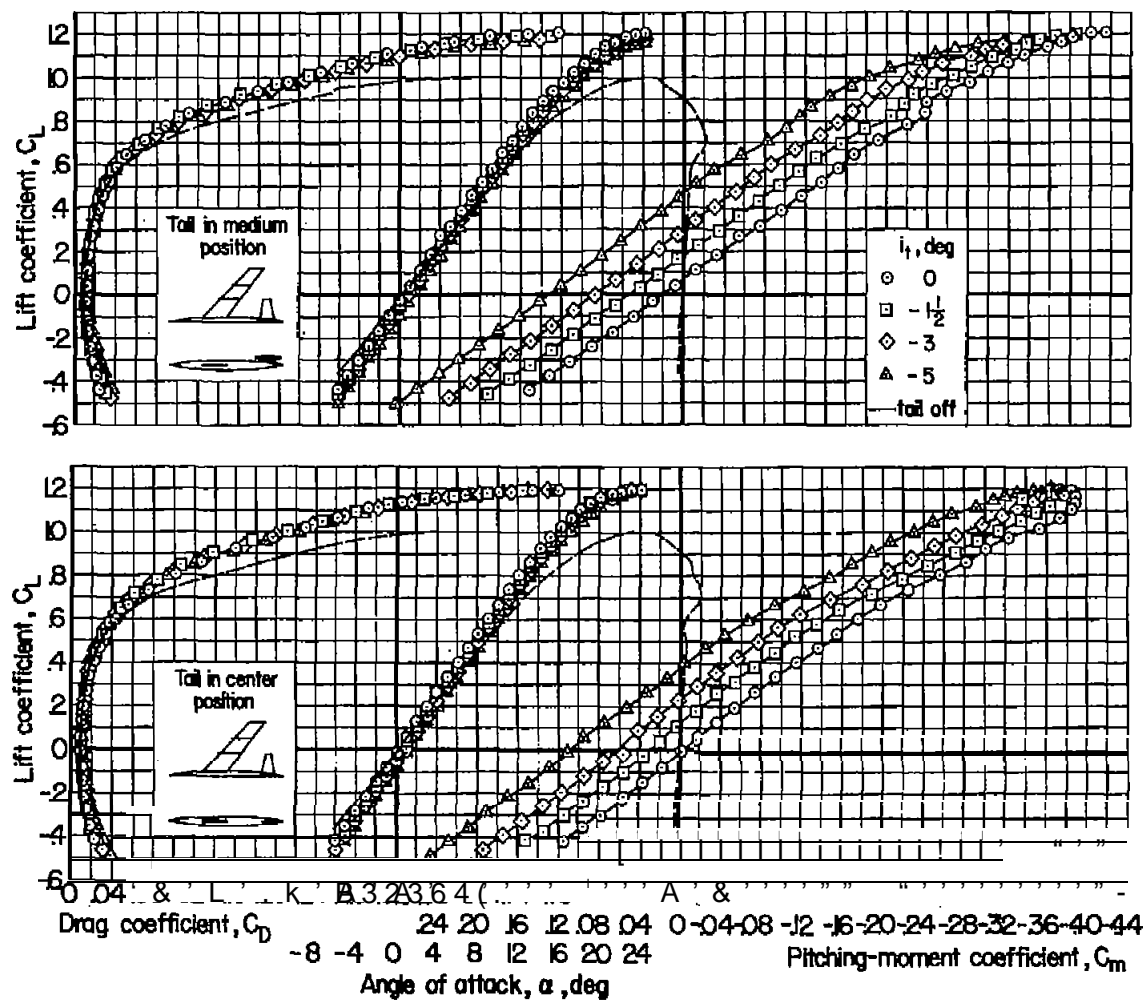
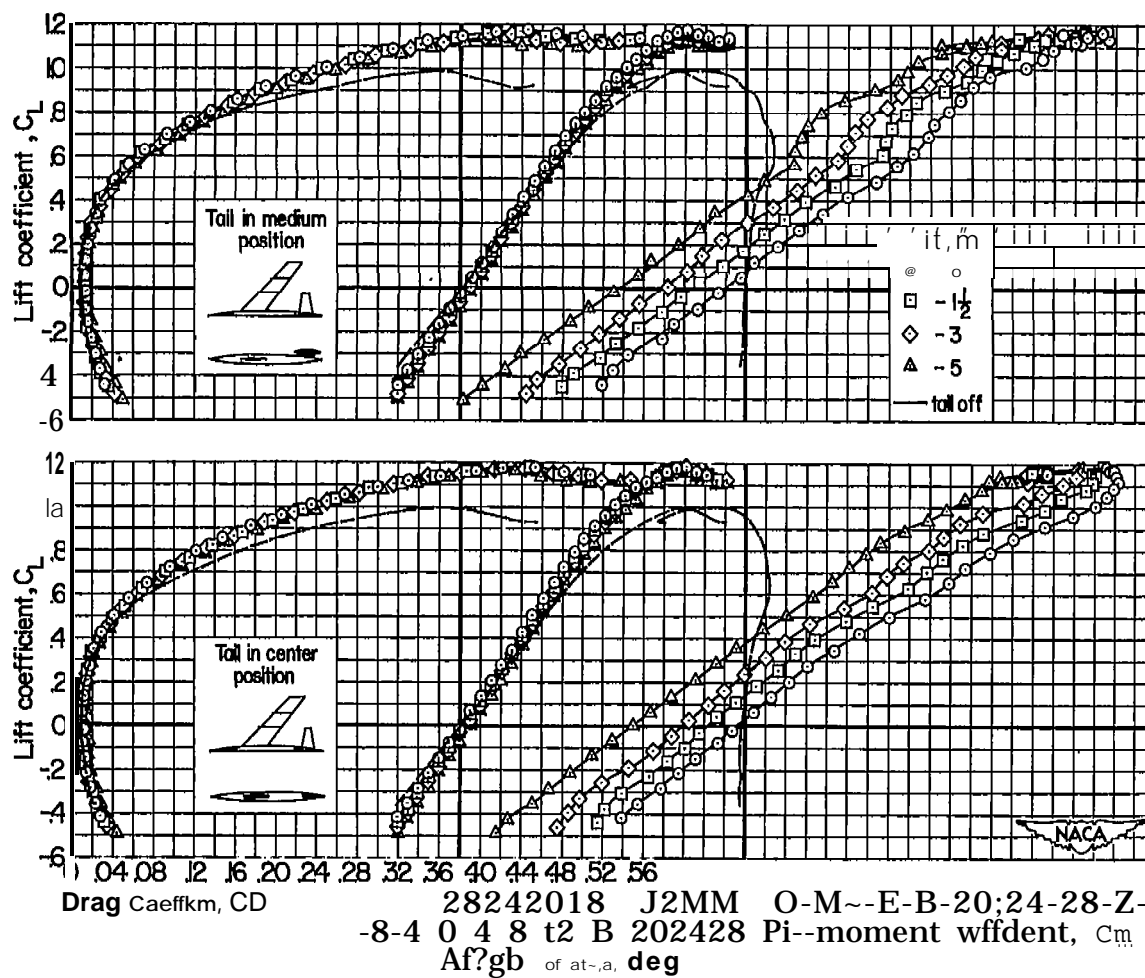
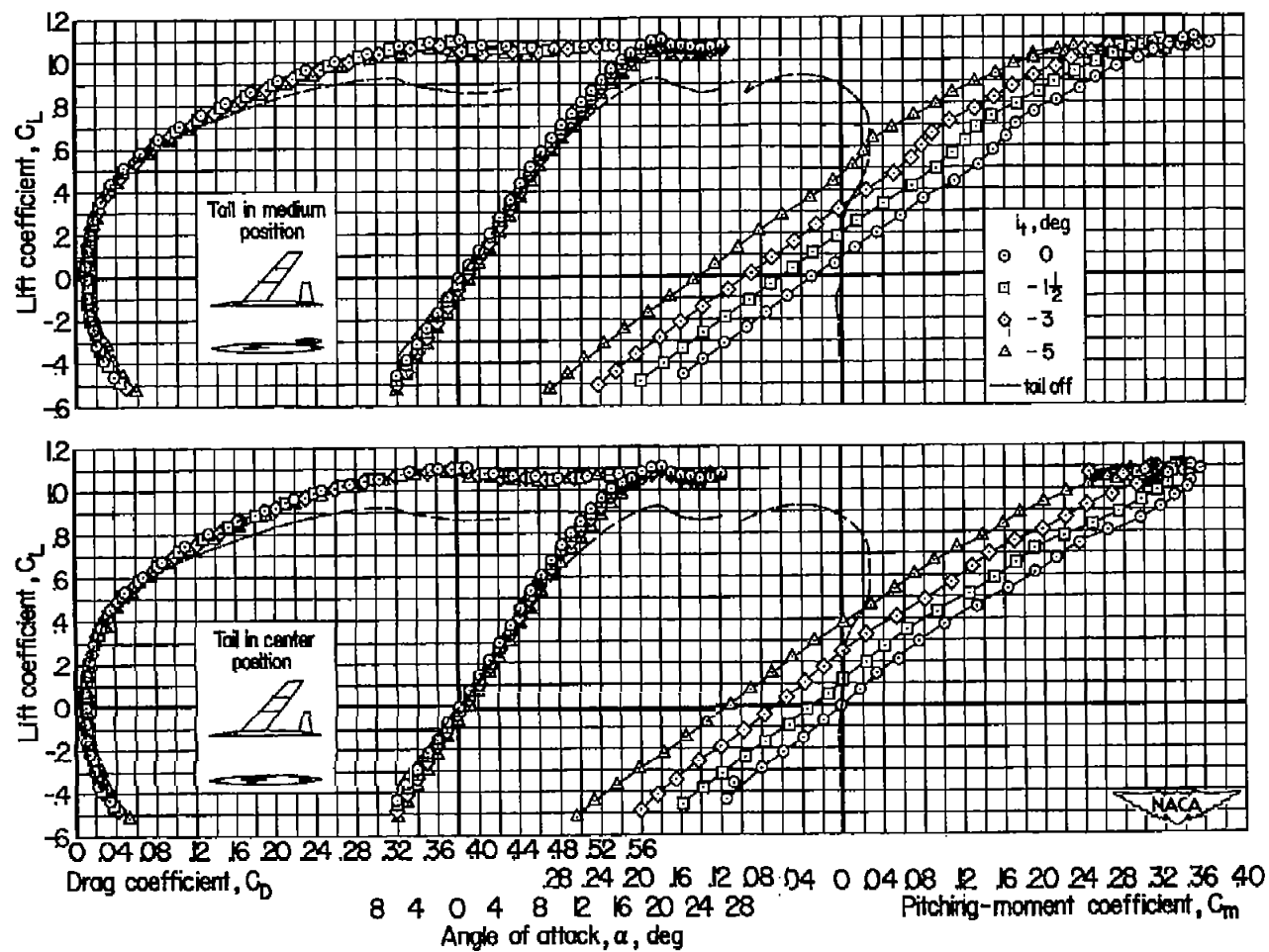


Figure 19. - The aerodynamic characteristics of the model with fences with the tail in the medium and center position at a Reynolds number of 10,000,000; $H = 0.5$.



(a) $M = 0.8$

Figure 20. - The aerodynamic characteristics of the model tith fences and the tail in the medium and center positions at a Reynolds number of 2,000,000,



(b) $M = 0.8$

Figure 2. Continued.

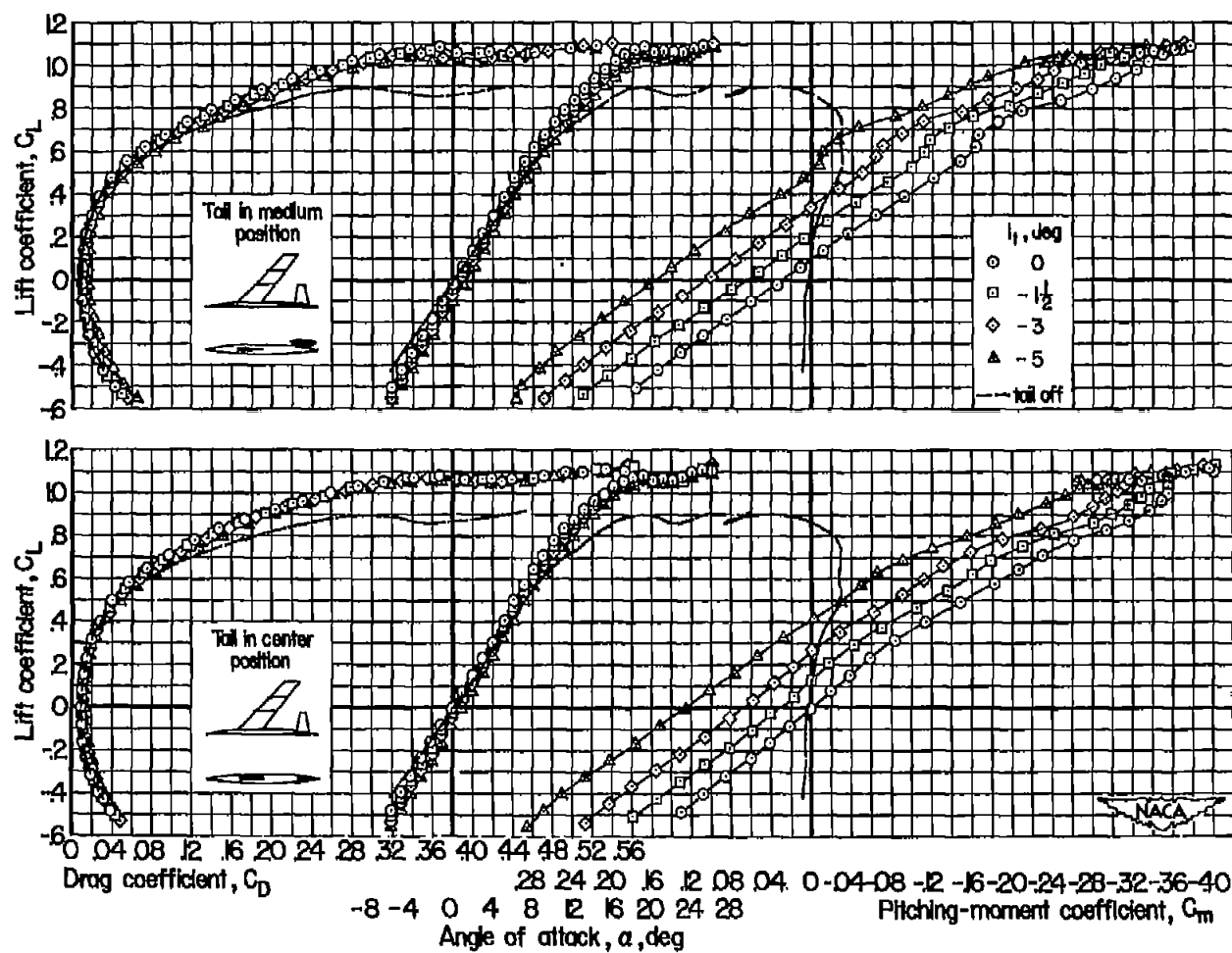
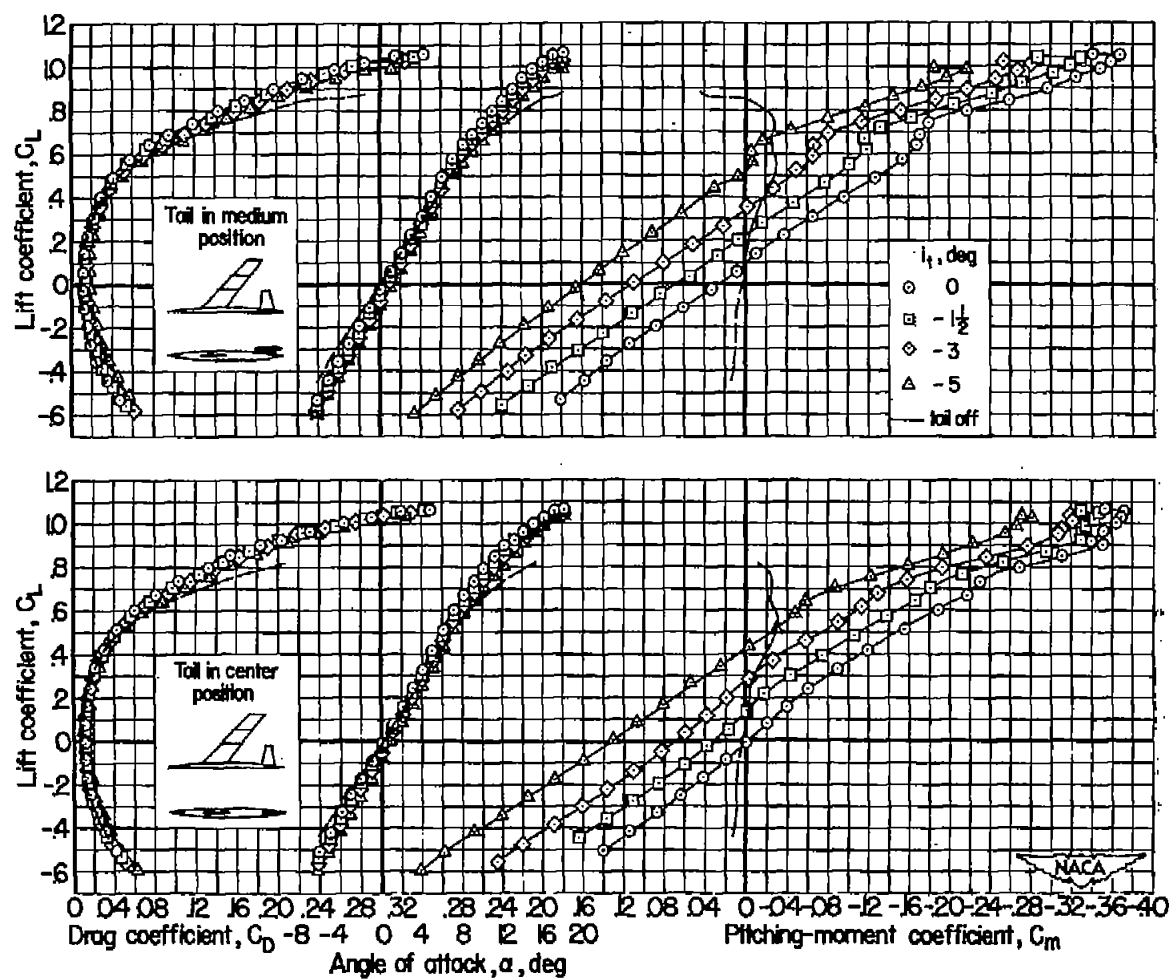
(c) $M = 0.80$

Figure 20.- Continued.



(d) $M = 0.0$

Figure 20. - Contj.nued.

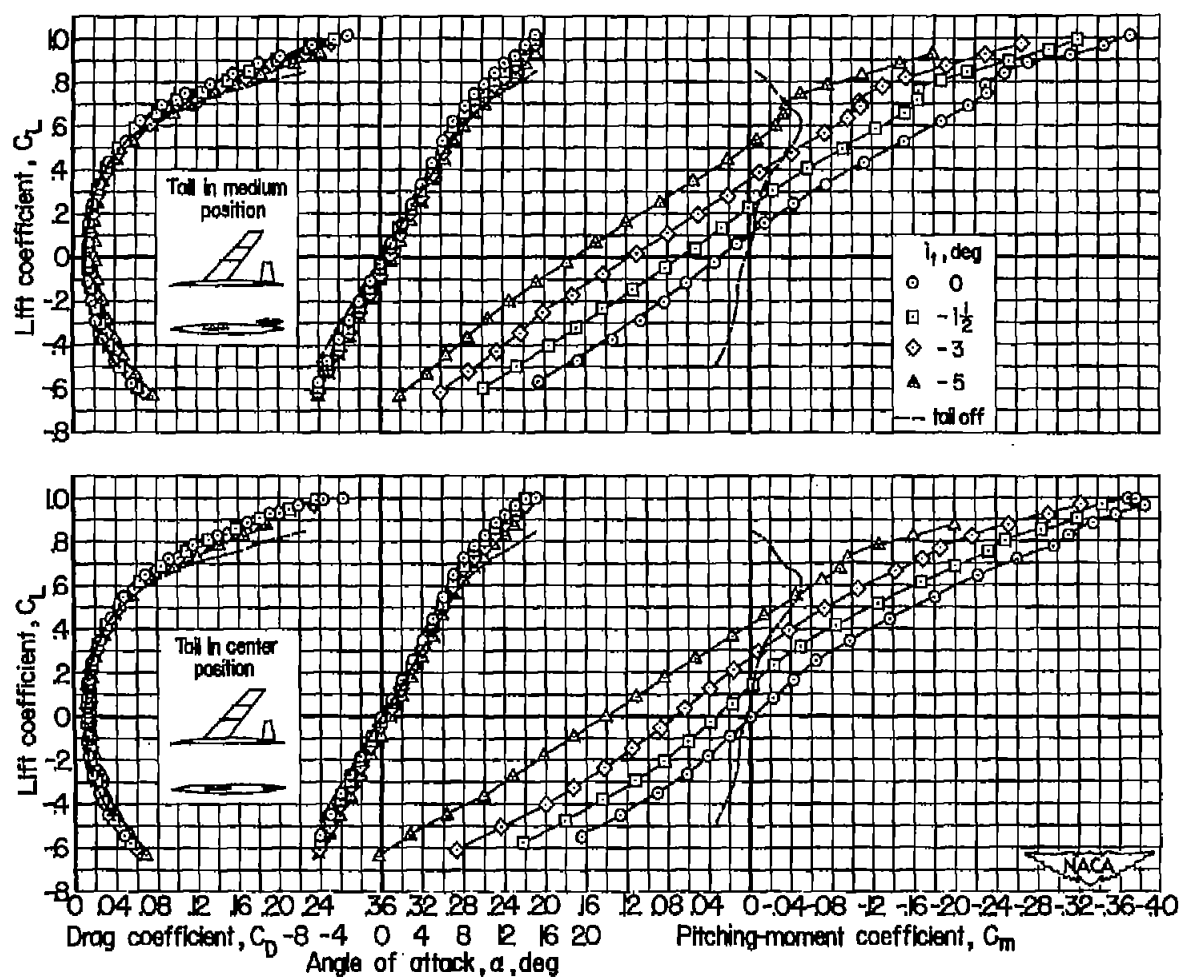
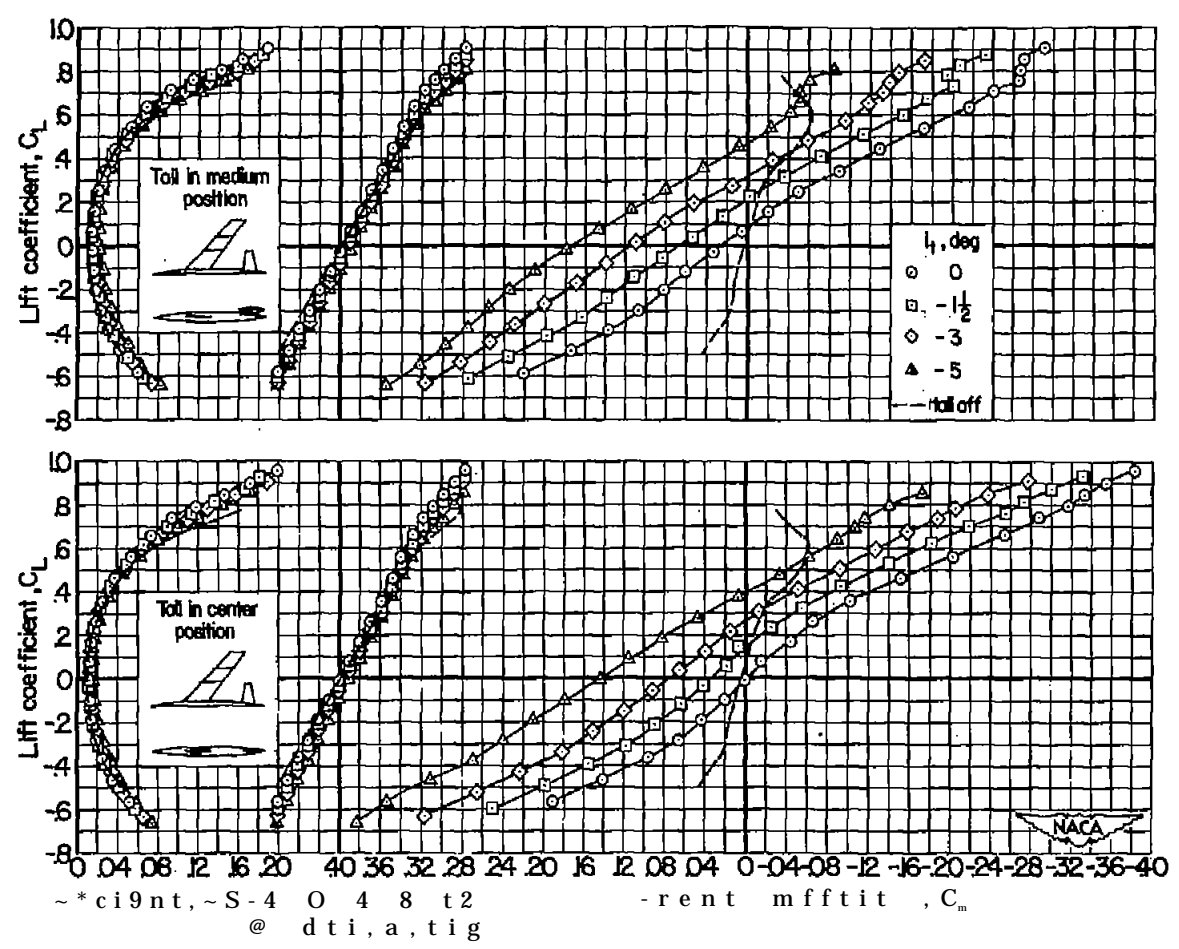
(e) $M = 0.90$

Figure 20. - Continued.

CONFIDENTIAL



(f) $M = 0.0$

FiP ~.- Concluded.

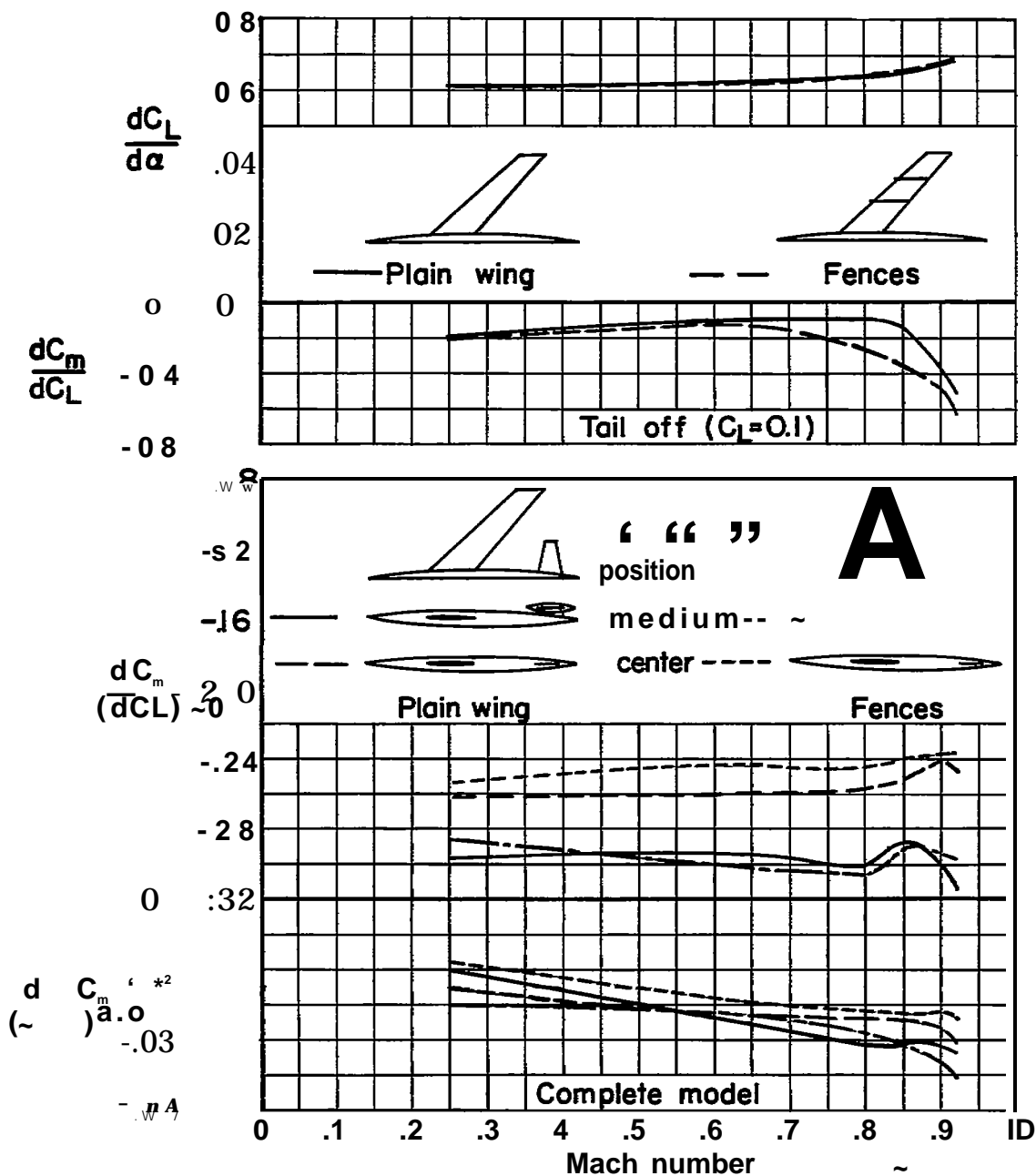


Figure 21. - The variation with Mach number of lift-curve slope, pitching-moment-curve slope, and stabilizer effectiveness; $R = 2,000$.

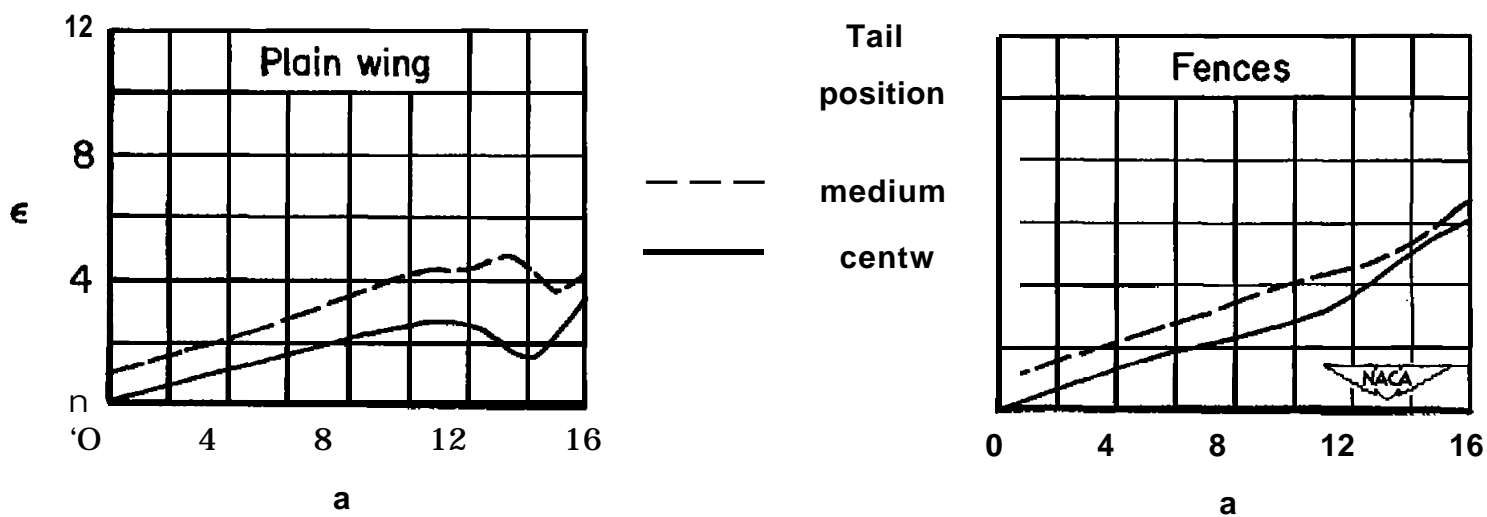


Figure 22. Comparison of effective drag coefficient at the tail with and without fences at a Reynolds number of 10,000; $M = 0.5$.

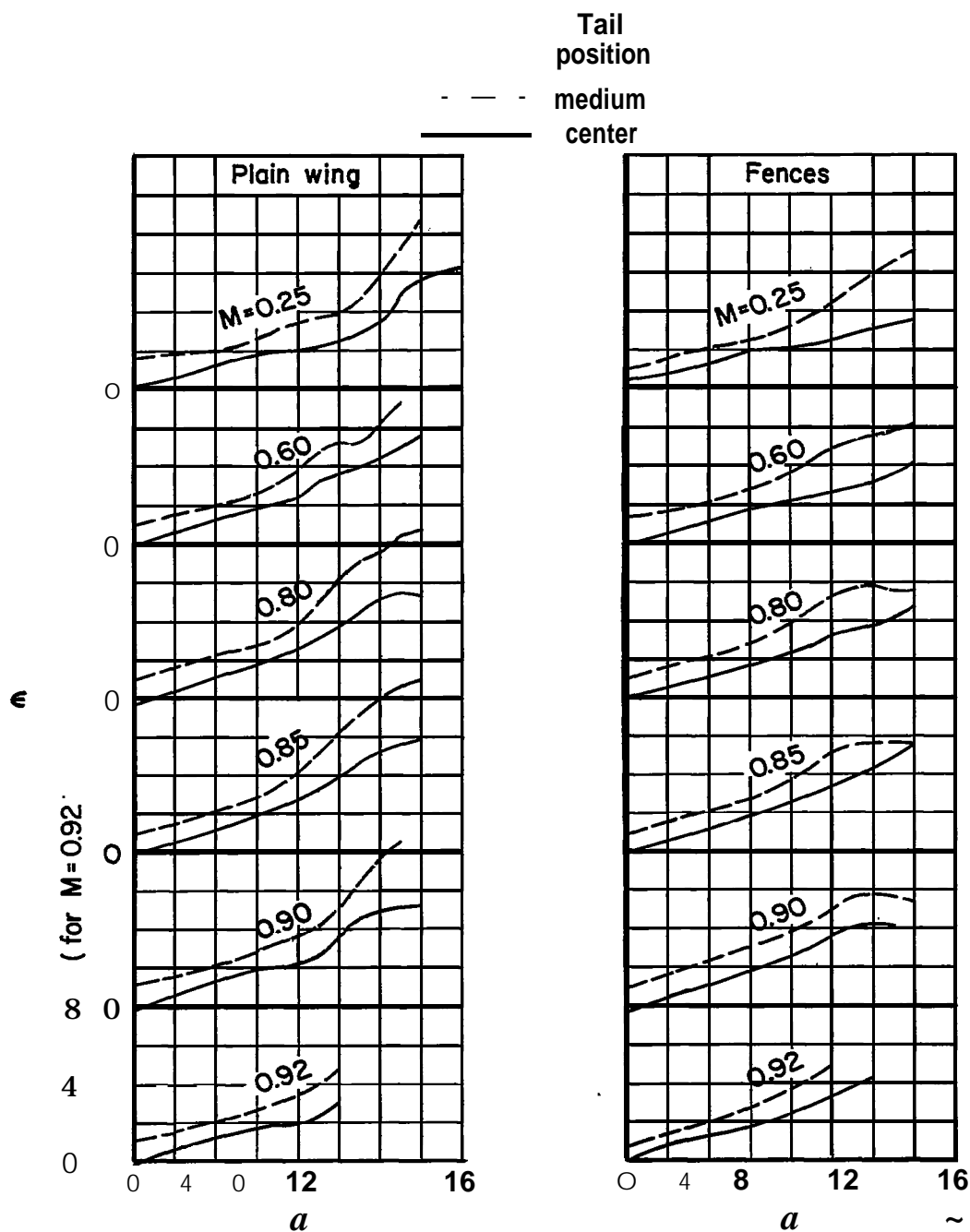


Figure 23. - The variation of effective downwash at the tail with angle of attack for the model with and without fences at various Mach numbers; $R = 2,000, \sim 0$.

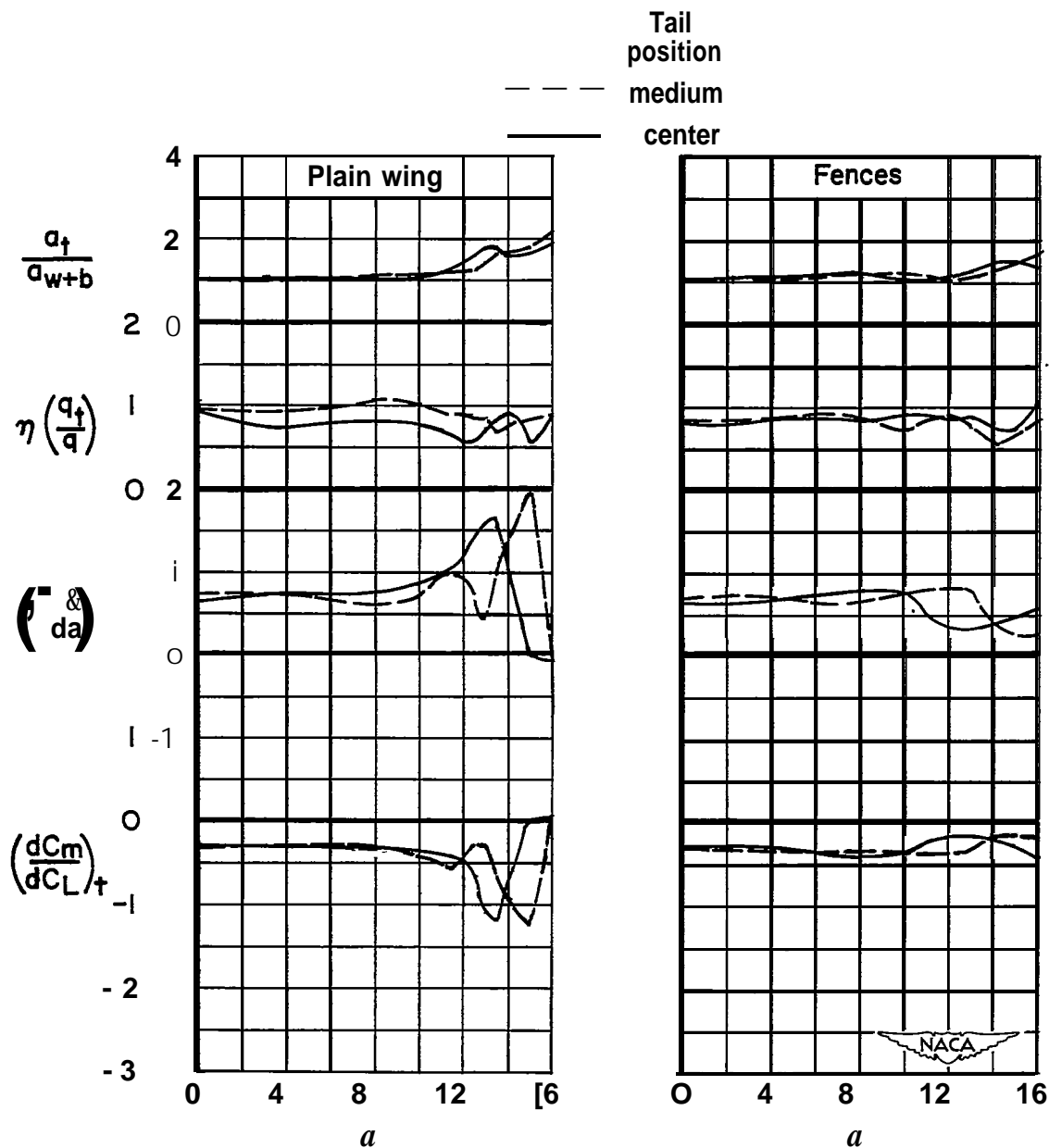


Figure 24. - The variation with angle of attack of the tail stability parameter and the factors affecting the stability contribution of the horizontal tail at a Reynolds number of 10,000,000; $M = 0.25$.

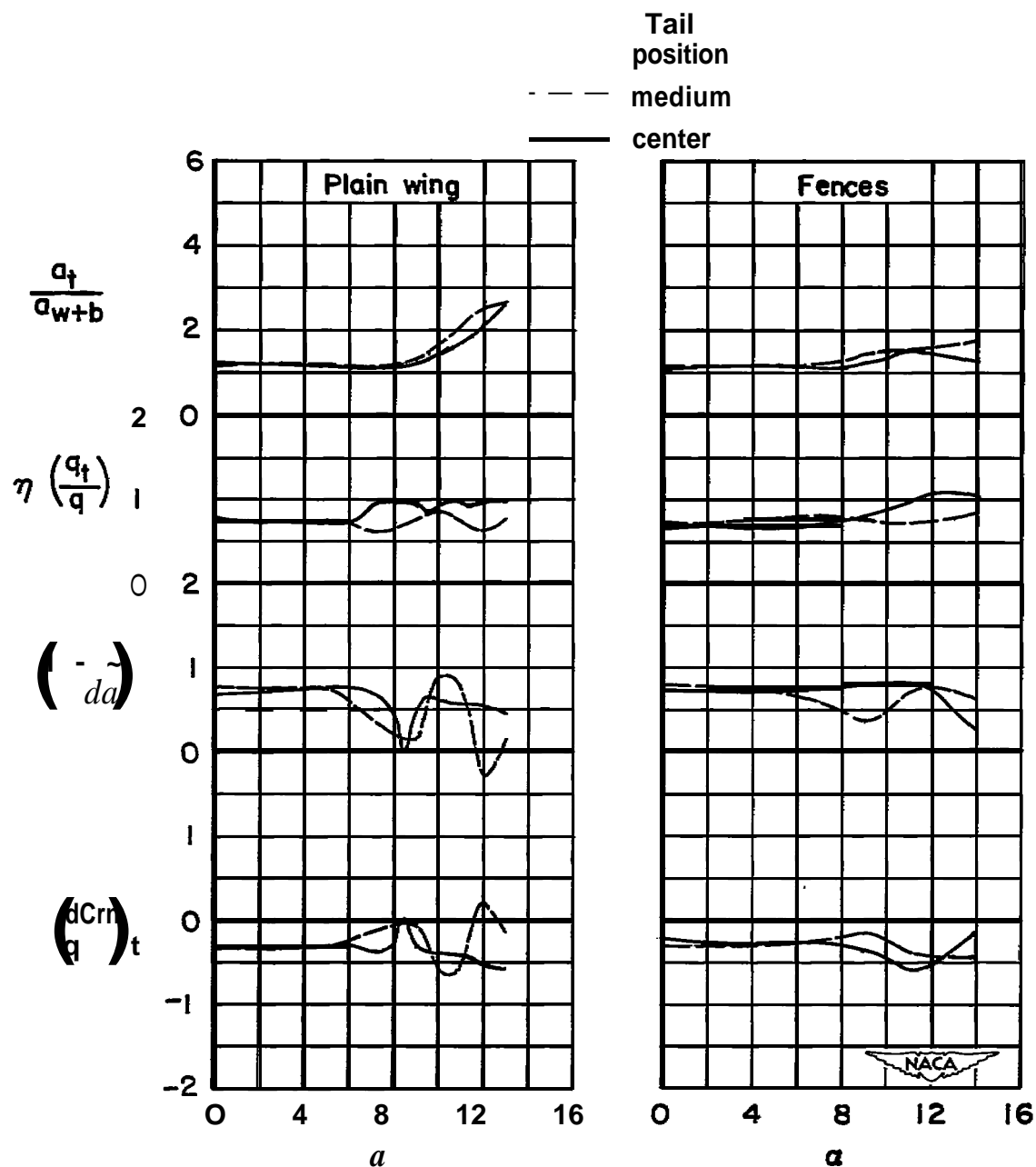
(a) $M = 0.60$

Figure ~. - me vafiation with angle of attack of the tail stability
parmeter and the factors affecting the stability contribution of the
horizontal tail; $R = 2,000,000$.

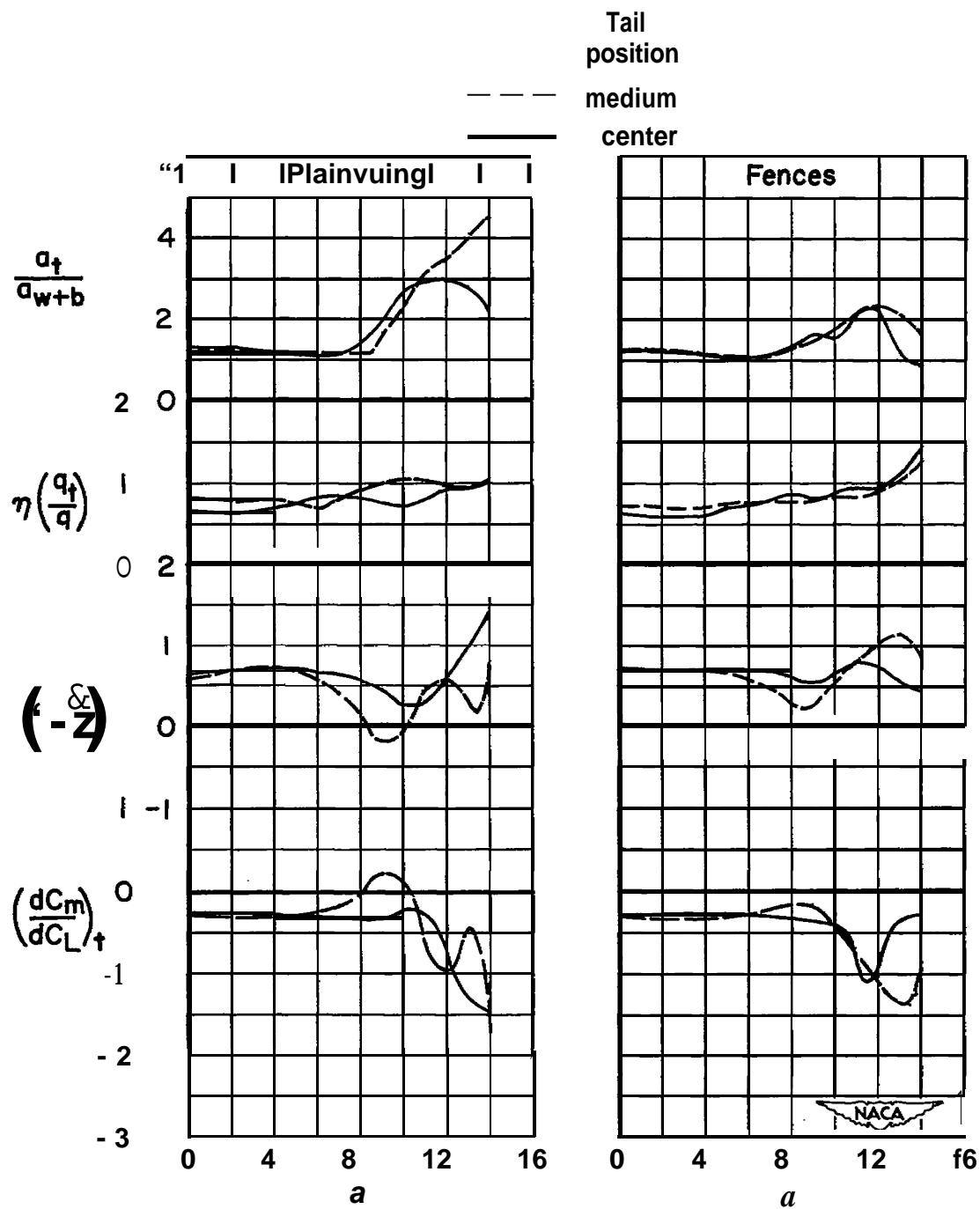
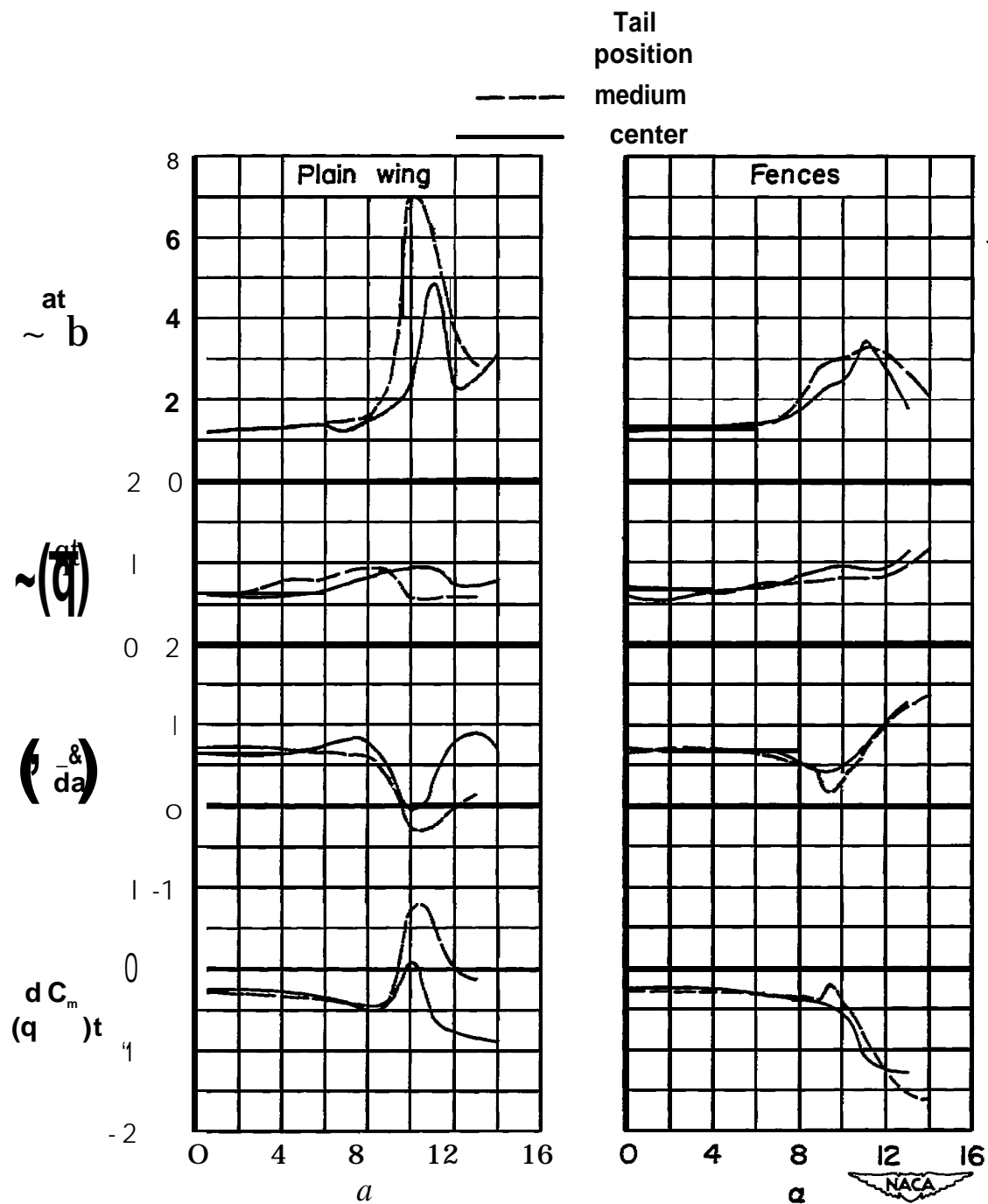
~~CONFIDENTIAL~~

Figure ~. - Continued.

~~CONFIDENTIAL~~

(c) $M = 0.5$

File ~. - Concluded.

~~CONFIDENTIAL~~

~MA RM A54K09

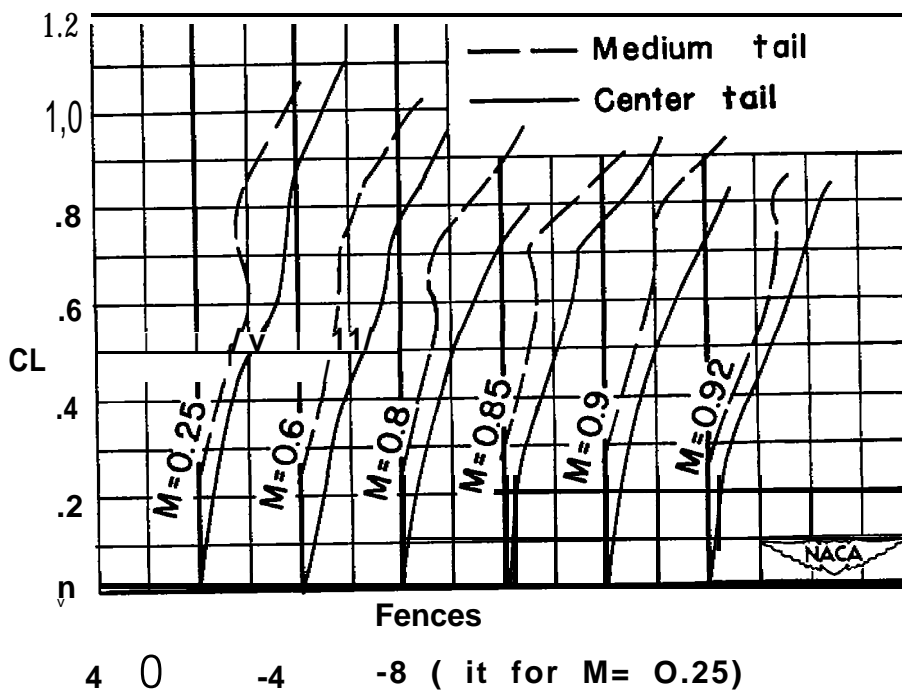
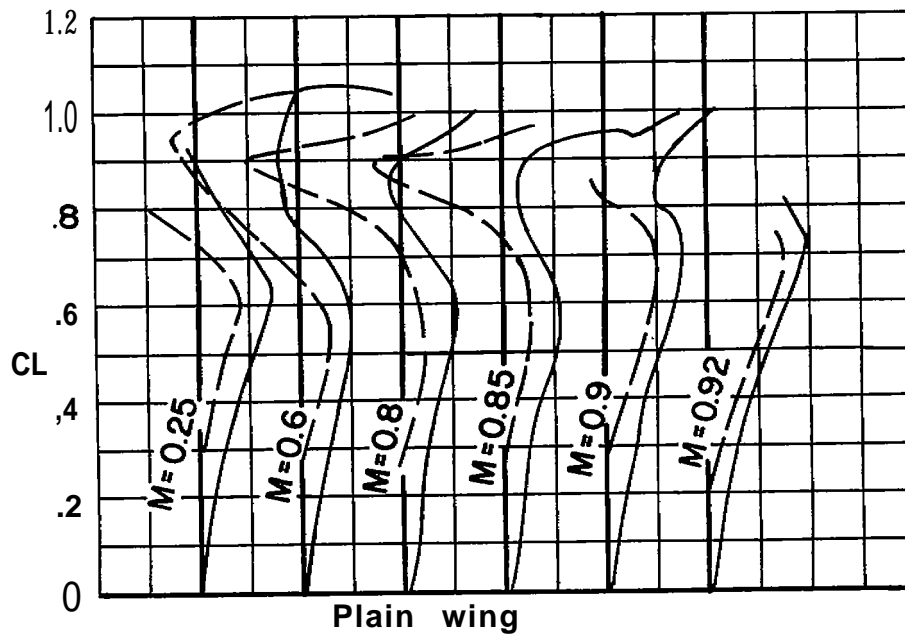


Figure 26. - The variation of tail incidence for longitudinal balance with lift coefficient at various Mach number; e.g., at $M=0.4$ & $R = 2,000,000^*$

~~CONFIDENTIAL~~